Synthetic Bilayer Membranes: Molecular Design, Self-Organization, and Application

By Toyoki Kunitake*

Lipid bilayers are a most central building block of the biological molecular organization. Their two-dimensional self-assembly is essential to the generation of biological shapes and sizes on the molecular level. The observation that a totally synthetic amphiphile in water is spontaneously assembled to a bilayer structure suggested that bilayer formation is a general physicochemical phenomenon that is not restricted to particular structures of biolipid molecules. Bilayer formation is now observed for a large variety of synthetic amphiphiles which contain one, two, three, or four alkyl tails. The flexible alkyl tail may be replaced by perfluoroalkyl chains. The supramolecular structures obtained therefrom can be related to the component's molecular structure in many cases. The structural variety and the ease of molecular design make the synthetic bilayer an attractive vehicle for organizing covalently bound functional units and guest molecules. In addition, stable monolayers on water, planar lipid membranes (BLM), and free-standing cast films are obtainable because of the self-assembling property of bilayer-forming compounds. These molecular organizations display common supramolecular features. The use of the cast film as a molecular template provides exciting potential for the production of novel two-dimensional materials.

1. Introduction

Biomembranes provide one of the most important structural units in the organization of the biological cell. In 1964 Bangham and Horne[1] demonstrated that the bilayer structure forms spontaneously from aqueous lipid dispersions, thus establishing that among the constituents of biomembranes, the lipid bilayer plays a most central role in maintaining biological molecular organization. Their discovery led to extensive research on biomembrane mimics and liposomes.

Attempts to prepare a bilayer assembly from amphiphilic compounds different from the natural lipid were conducted concurrently. For example, Gebicki and Hicks observed formation of globular aggregates ("Ufasome") when they dispersed thin films made of oleic acid and linoleic acid in water.[2] Hargreaves and Deamer[3] obtained vesicles by codispersion of fatty acids and higher alcohols. Vesicular aggregates have also been described for 1:1 mixtures of saturated fatty acids (C_{12} to C_{18}) and lysolecithin. However, these aggregates were not sufficiently stable and provided no definite evidence for the isolated bilayer structure.[**]

Many investigators have discussed reasons why some of the polar lipid molecules can form two-dimensionally aligned assemblies. For example, Brockerhoff interpreted the structural features of membrane lipids in terms of a tripartite structure: hydrophobic aliphatic double chain, hydrophilic head group, and the (hydrogen belt) region linking these two moieties.[4] Tanford proposed that bilayer formation can be accounted for by purely geometrical consideration of the volume of the hydrophobic core and the surface area occupied by the head group in membrane lipids.[5] Israelachvili, Mitchell, and Ninham[6] emphasized the role of molecular geometry in determining the structures of lipidic or amphiphilic assemblies and asserted that the packing constraint of a component molecule decided the surface curvature, that is, the morphology of resulting molecular aggregates.

These theories certainly explain the formation of bilayer membranes from biological lipids; however, they do not provide guiding rules that enable us to design novel bilayer-forming compounds.

When we set out to develop new bilayer-forming compounds in 1976, we assumed that the unique structure of the polar head group of biolipid molecules was determined by the biosynthetic and physiological requirements rather than by the physical chemistry of membrane formation. Our first candidates were, therefore, simple double-chain ammonium salts. Didodecyldimethylammonium bromide (**1**, $n = 12$)

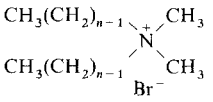

1

gives a clear aqueous dispersion by sonication. When this dispersion was negatively stained by uranyl acetate and observed by electron microscopy, the formation of single- and multiwalled vesicles with a layer thickness of 30–50 Å was recognized (Fig. 1). Their aggregation characteristics such as critical aggregate concentration and molecular weight were consistent with a bilayer vesicle. This result was the first example of a totally synthetic bilayer membrane.[7]

The exceptional behavior of double-chain ammonium salts as aqueous dispersions has been noted many years ago. Ralston, Eggenberger, and DuBrow studied the aggregation behavior of these salts by conductometry and found an unusual dependence of the equivalent conductivities at low concentrations.[8] Kunieda and Shinoda prepared the phase

[*] Prof. Dr. T. Kunitake
Department of Chemical Science and Technology, Faculty of Engineering
Kyushu University, Fukuoka 812 (Japan)

[**] Spontaneous vesicle formation in aqueous mixtures of cationic and anionic single-chain surfactants was described recently: E. W. Kaler, A. K. Murthy, B. E. Rodriguez, J. A. N. Zasadzinski, *Science* **1989**, *245*, 1371.

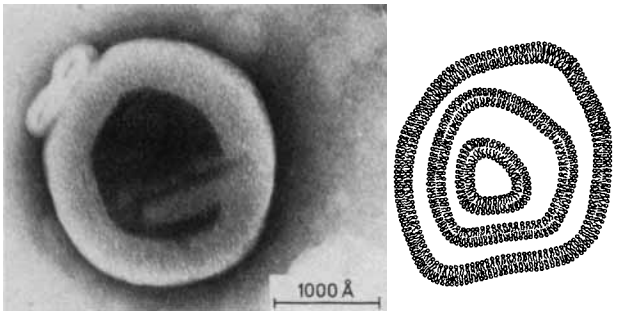

Fig. 1. Electron micrograph (left, negatively stained with UO_2^{2+}) and schematic illustration (right) of the multiwalled vesicle of **1** ($n = 12$).

diagram of these ammonium salts and indicated the transitions between molecular dispersion, liquid crystalline dispersion, and liquid crystal.[9] These dispersions were, however, never referred to as bilayer membranes.

It is important to make a distinction between liquid crystalline dispersions and bilayer membranes. As pointed out by Gray and Winsor,[10] it is the intermicellar forces—that is, the lattice forces—rather than forces from jointing or close packing which determine the viscosities and stabilities of the mesophases. In contrast, a bilayer membrane should be able to exist as an isolated entity without relying on the lattice forces for maintaining its structural integrity. The presence of lamellar multibilayer structures does not warrant the formation of bilayer membranes. We need to show the existence of isolated bilayer structures. The formation of bilayer membranes requires a self-assembling property greater than that of liquid crystalline dispersions.

In the following, we review the molecular design of bilayer-forming molecules, their aggregate morphologies, and some applications. Instead of attempting to prepare an exhaustive catalogue of those compounds, we present the design principle of component amphiphiles and the molecular organization they produce. The molecular design will be discussed in terms of the module concept given in Figure 2. This concept can cover most, if not all, of the types of bilayer-forming compounds. The functional aspects will be discussed only briefly in the last section.

Excellent reviews on various aspects of synthetic bilayer membranes have been published: Fendler prepared an extensive list of amphiphiles that are capable of bilayer formation (up to 1982);[11] routes to functional vesicle membranes have been discussed by Fuhrhop and Mathieu;[12] an extensive review on polymeric bilayer membranes was published by Ringsdorf, Schlarb, and Venzmer[13] in this journal. The last topic is, therefore, not discussed here.

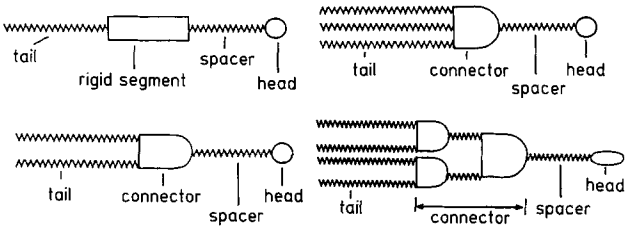

Fig. 2. Structual elements (modules) of bilayer-forming amphiphiles.

2. Bilayer Membranes of Double-Chain Amphiphiles

2.1. Molecular Design and Aggregation Behavior

Many double-chain amphiphiles have been synthesized as analogues of natural lecithin molecules, and their bilayer formation examined. The required molecular modules are tail, connector, spacer, and head groups.

Subsequent to our initial finding,[7] we conducted a systematic survey on the aggregation behavior of dialkylammonium salts with different tail lengths (Table 1).[14] All the

Table 1. Aggregation behavior of dialkyldimethylammonium bromides $R^1R^2Me_2N^+Br^-$ (**1**) [a].

R^1	R^2	Solution [b]	Electron Micrograph	M [c]	T_c [d] [°C]
$C_{22}H_{45}$	$C_{22}H_{45}$	colloidal	lamella		70
$C_{18}H_{37}$	$C_{18}H_{37}$	colloidal	lamella	10^7	45
$C_{16}H_{33}$	$C_{16}H_{33}$	colloidal	lamella & vesicle	–	
$C_{14}H_{29}$	$C_{14}H_{29}$	colloidal	vesicle & lamella	5×10^6	16
$C_{12}H_{25}$	$C_{12}H_{25}$	clear	vesicle	7×10^5–1×10^6	n.d. [e]
$C_{18}H_{37}$	$C_{16}H_{33}$	colloidal	lamella	2×10^8	31
$C_{18}H_{37}$	$C_{14}H_{29}$	colloidal	vesicle & lamella		
$C_{18}H_{37}$	$C_{12}H_{25}$	clear	vesicle	8×10^6	n.d. [e]
$C_{18}H_{37}$	$C_{10}H_{21}$	clear	vesicle	3×10^6	
$C_{18}H_{37}$	C_8H_{17}	clear	unstructured		
$C_{16}H_{33}$	CH_3	clear	unstructured		

[a] The data are mostly taken from [14] and appended by later experiments. [b] Appearance of the 10 mM solution after sonication. [c] Molecular weight by light scattering. [d] Phase transition temperature. [e] Not determined.

Toyoki Kunitake was born in 1936 in Kurume-shi, Fukuoka-ken, Japan. After completing his M.Sc. in the Faculty of Engineering at Kyushu University in 1960, he studied chemistry under C. C. Price at the University of Pennsylvania, graduating with a Ph.D. degree in 1962. He then spent a year as post-doctorate with C. G. Nieman at the Department of Chemistry, California Institute of Technology, before returning to Kyushu as Associate Professor in 1963. He was promoted to Professor in the Faculty of Engineering in 1974. Besides the field of synthetic bilayer membranes his research interests cover ultrathin films and Langmuir–Blodgett films, surface monolayers, and supramolecular aggregates.

double-chain compounds give colloidal solutions by sonication, and the molecular (aggregate) weights determined by light scattering lie between 10^6 and 10^7. Electron microscopy indicates the presence of vesicles (Fig. 1) and lamellae (Fig. 3), when both alkyl chains are at least ten carbon atoms long. Their layer thicknesses are 30–40 Å, in agreement with

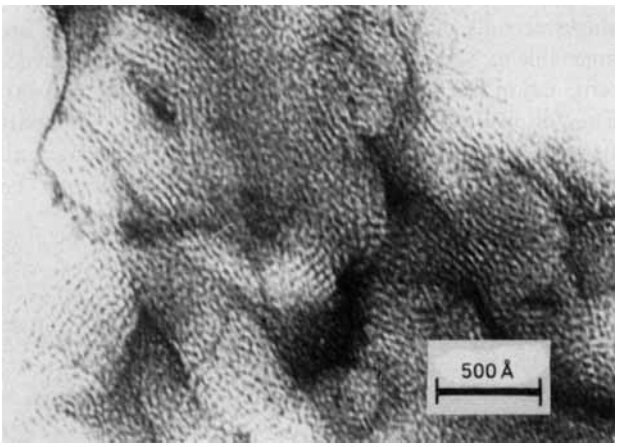

Fig. 3. Electron micrograph (negatively stained with UO_2^{2+}) of lamellar bilayers of **1** ($n = 14$).

the bilayer assemblage. Detection of the gel → liquid crystal phase transition by differential scanning calorimetry (see Section 2.3) strongly suggests the presence of aligned alkyl chains in the aggregate. These ammonium bilayers were extensively characterized.[15–18] The aggregate morphology is naturally affected by the method of dispersion.[17] Carmona-Ribeiro and Chaimovitch reported that large unilamellar vesicles (diameter, 0.5 μm) were obtainable by the solvent vaporization method.[19]

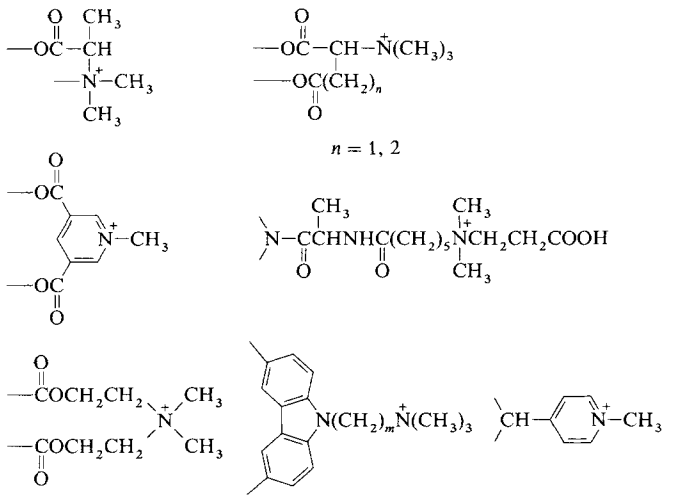

Fig. 4. Connectors of double-chain ammonium amphiphiles [21–25].

The dimethylammonium head can be modified by other substituents or replaced by the sulfonium group.[20] The connector portion that links the hydrophobic alkyl chains and the hydrophilic head group can be varied (Fig. 4). The major function of this unit is to help promote alignment of the alkyl chains. In the dialkyldimethylammonium salts of Table 1, the ammonium head group is directly bonded to alkyl tails without spacer units. A spacer unit that intervenes between the head group and the connector unit exerts significant influence on the molecular orientation in the bilayer. As discussed in Section 6, the length of the methylene chain functioning as spacer is critical in formation of helical superstructures.

Double-chain amphiphiles with anionic head groups form bilayer membranes. Examples with sulfonate (**2**), phosphate (**3**), and carboxylate (**4**) head groups are given in Table 2.[26]

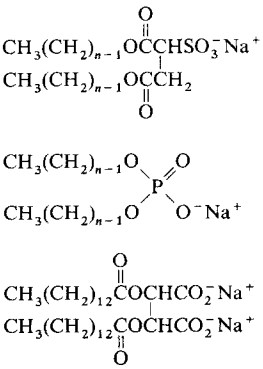

Stable bilayer membranes are formed again when the alkyl chain contains more than ten carbon atoms. The presence of vesicles and lamellae is confirmed by electron microscopy, and their molecular weights are 10^6–10^7. Mortara et al.[27] similarly noted vesicle formation from dihexadecyl phosphate at an early stage in this research.

Table 2. Aggregation behavior of anionic, dialkyl amphiphiles [26] [a].

Compound	Solution	Electron Micrograph	M	T_c [°C]
2 ($n = 16$)	colloidal	lamella	–	45
2 ($n = 12$)	colloidal	large vesicle	2.2×10^7	28
2 ($n = 10$)	clear	large vesicle	1.9×10^6	
3 ($n = 16$)	colloidal	lamella	1.2×10^7	67
3 ($n = 12$)	colloidal	vesicle	2×10^7	33
3 ($n = 10$)	clear	vesicle	4.4×10^6	
4 ($m = 13$)	slightly turbid	vesicle		

[a] See footnotes to Table 1.

The oxyethylene oligomer is conveniently used for preparing nonionic, bilayer-forming compounds.[28] The aggregation behavior of these compounds is summarized in Table 3 for **5** and **6**. In the case of **5** ($n = 8$), bilayer formation is not detected and the molecular weight of the aggregates (ca. 10^5) is smaller than those for typical bilayer aggregates ($> 10^6$).

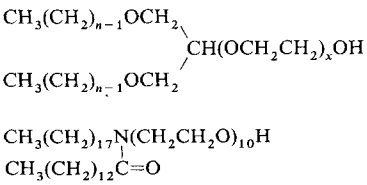

Table 3. Aggregation behavior of nonionic amphiphiles [28] [a].

Compound (n, x)	cmc [b] [μ M]	Electron Micrograph	M	T_c [°C]
5 (8, 6)		unstructured	5×10^5	
5 (8, 10)	50	unstructured	4×10^5	
5 (8, 12)	60	unstructured	6×10^5	
5 (12, 10)	2	irregular vesicles	turbid	
5 (12, 15)	2	vesicles and lamellae	1.2×10^7	n.d.
5 (12, 28)	1	lamellae	1.2×10^7	
5 (14, 15)		vesicles		22 [c], 30
5 (16, 15)			turbid	40–44
5 (16, 12)	1	paired bilayers	2.7×10^7	41
5 (16, 30)	1	lamellae	4.6×10^7	n.d.
5 (18, 15)		disks		51, 55 [c]
6		fragments of lamellae	1.5×10^7	

[a] See also footnotes to Table 1. [b] Critical aggregate concentration. [c] Major DSC peak.

The longer chain analogues **5** ($n = 12$) and **5** ($n = 16$) produce bilayer aggregates which exhibit different morphologies. For instance, **5** (12, 15) gives single-compartment vesicles, whereas **5** (16, 15) produces paired bilayers (Fig. 5).

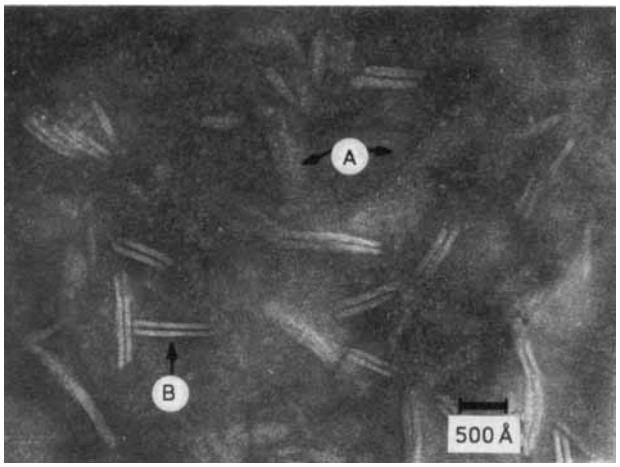

Fig. 5. Electron micrograph of an aqueous dispersion of **5** (16, 15). A top view (arrow A), and a side view (arrow B) of paired bilayers.

Zwitterionic groups such as **7**, **8**, **9**, and **10** were also used as the head group of double-chain amphiphiles.[23, 28]

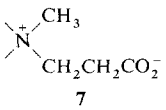

7

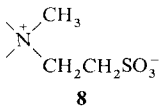

8

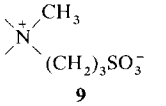

9

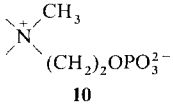

10

2.2. Molecular Alignment in Bilayer Assemblage

The detailed molecular arrangement in some of the synthetic bilayers mentioned above has been elucidated by X-ray crystallography. Kajiyama et al.[29] estimated the bilayer thickness of a series of simple double-chain ammonium amphiphiles **1** from widths between dark striations in electron micrographs of negatively stained samples. They also determined the layer thickness of powder samples. Comparisons of these data with the molecular lengths suggested that the component molecules were tilted with respect to the bilayer surface by 32 to 47° depending on the alkyl chain length.

Okuyama et al. succeeded for the first time in preparing single crystals of a synthetic bilayer compound that are amenable to X-ray structural analysis.[30] The structure determination has been conducted for **1** ($n = 14$, 16, and 18). They all give intrinsically identical structures,[31, 32] apart from the chain length. As an example, the packing structure of the monohydrate of **1** ($n = 18$) is given in Figure 6. The

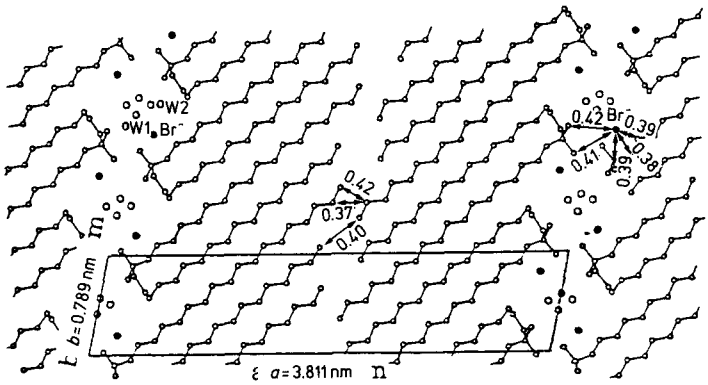

Fig. 6. The packing structure of a single crystal of the monohydrate of **1** ($n = 18$).

most important aspects in this structure are as follows: a) Br^- and N^+ centers form a hydrophilic plane parallel to the bilayer surface; b) the component molecules are tilted by 45° relative to the bilayer surface; c) one of the octadecyl chains assumes the *trans* zigzag conformation, whereas the other chain shows a folded conformation (*ggtgg*) near the hydrophilic group and the *trans* zigzag conformation towards the alkyl chain end. The chain tilting is caused by the balance between the molecular cross-sections of the hydrophobic portion (40 $Å^2$ for two methylene chains) and the hydrophilic portion (57 $Å^2$ for the *bc* plane of the unit lattice). This packing structure is very similar to that found for phosphatidylcholine.[11] The tilt structure was always found for double-chain amphiphiles with the glutamate connector.[33, 114] It is noteworthy that the ammonium amphiphile with two identical chains assumes the unsymmetrical chain packing. This seems to be a common requirement of chain packing among double-chain amphiphiles in order to attain the two-dimensionality.

2.3. Phase Transition and Phase Separation

Phase transition and phase separation are the two, most fundamental properties related to bilayer assemblage. Phase transition is schematically illustrated in Figure 7.

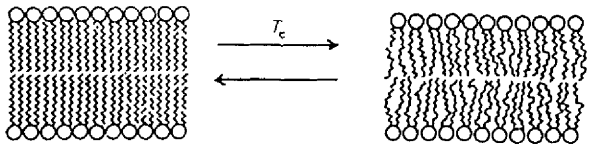

Fig. 7. A schematic illustration of the phase transition, crystalline $\rightleftharpoons$ liquid crystalline at the phase transition temperature T_c.

One of the simplest bilayer-forming amphiphiles, **1** ($n = 18$) shows a remarkably complex phase behavior.[9, 34] We are interested here only in dilute dispersions. The gel→liquid crystal phase transition is commonly observed for dilute aqueous dispersions of double-chain amphiphiles. Figure 8 depicts DSC (differential scanning calorimetry) thermograms for aqueous dispersions of **1** ($n = 12$, 14, 16, 18, and 22). The phase transition temperature, T_c, increases with increasing lengths of the alkyl tail. Many of the bilayer dispersions prepared by sonication give broader DSC peaks. The molecular organization in these well-dispersed samples may not be uniform. In contrast, DSC samples frozen to $-50\,^{\circ}C$ give sharper single peaks, probably because more regular, multilamellar dispersions are formed.

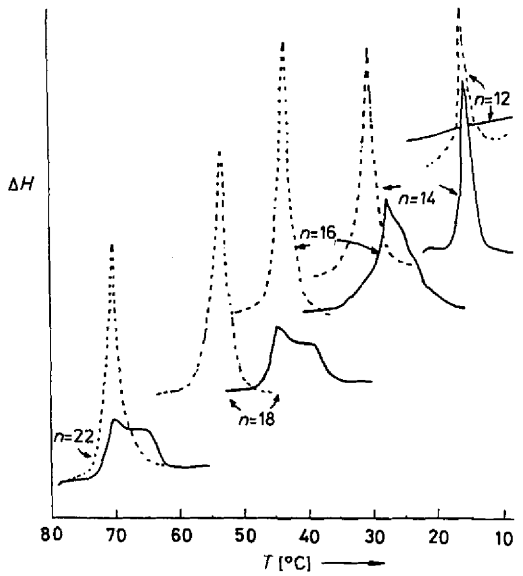

Fig. 8. DSC curves of bilayers of 1–2 wt% of **1** in water. — Samples prepared by the sonication method; - - - samples prepared by the dispersion method or the freezing method.

These data are consistent with the phase transition ranges estimated by other methods: reaction rates in the bilayer matrix, NMR line broadening of the crystalline bilayer, fluorescence spectral changes of probe molecules, turbidity changes, and the extent of positron annihilation.[35] The difference in T_c between the sonicated and frozen samples depends on the molecular structure of the component amphiphile, as shown in Scheme 1. In the case of the simple dimethyldioctadecylammonium amphiphile, **1** ($n = 18$), the sonicated sample has a T_c 9 °C lower than the frozen sample. In other dioctadecylammonium amphiphiles, which possess more complex head and/or connector groups, the differences are much smaller. Uniform bilayer organizations appear to be maintained when hydrogen bonding and/or dipolar interaction are expected between component molecules.

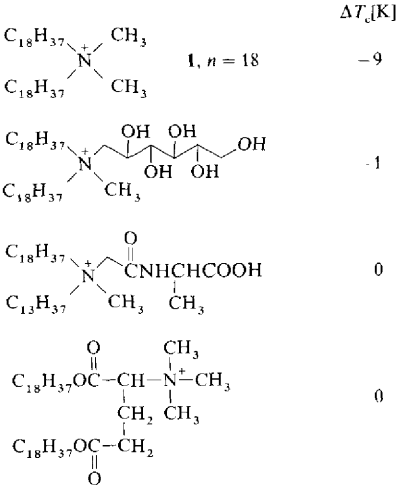

Scheme 1. Difference in T_c of aqueous dispersions of double-chain amphiphiles generated by sonication or freezing.

We compiled DSC date (T_c, enthalpy and entropy change) for the whole family of bilayer-forming, double-chain amphiphiles.[36, 37] The design of a novel bilayer with desired phase transition behavior is now possible. The correlations between this behavior and molecular structure are summarized as follows:

1) The entropy change of the phase transition falls within the range of 60–220 $JK^{-1}mol^{-1}$ for stable bilayers of all double-chain amphiphiles including natural lipids. This indicates that all phase transition processes are closely related (chain melting).

2) The variation of the DSC data can be discussed in terms of the structural element of component amphiphiles: a) T_c, ΔH, and ΔS values increase with increasing lengths of tails and spacers, except when diethanolamine is connector; b) enhanced interactions among connectors raise T_c values. However, the corresponding changes in ΔS are not straightforward; c) head-group interactions (electrostatic and/or hydrogen bonding) raise T_c. When the interaction is not very strong, the DSC data (T_c, ΔH and ΔS) for bilayers of different surface charges (cationic, anionic, and neutral) does not vary. Bulky substituents at the head group cause T_c lowering; d) the presence of flexible units (ether and ester) either in the tail or in the spacer leads to T_c lowering. A *cis* double bond (as in the oleoyl group) has the same effect.

Phase separation of synthetic bilayer membranes has been detected by the presence of the component peak in DSC, by λ_{max} shifts in absorption spectroscopy, and by excimer emission in fluorescence spectroscopy. An example of the absorption spectral method is shown in Figure 9.[38] Azobenzene-

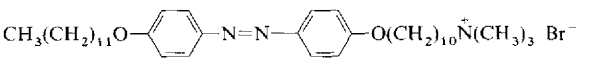

11

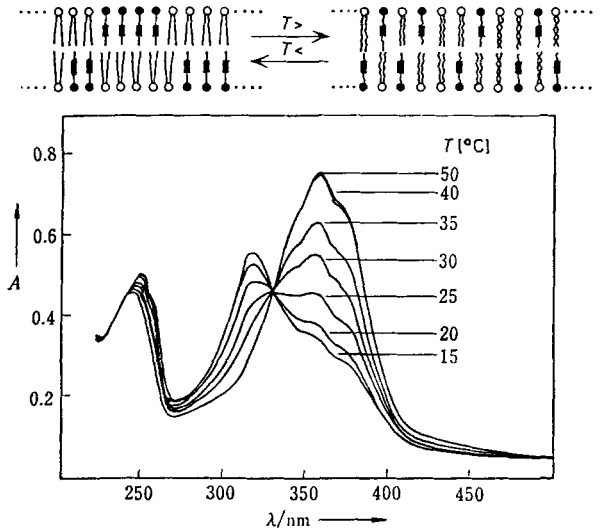

Fig. 9. Spectral changes in the absorption spectrum as a result of phase separation in a 1:10 mixed bilayer of **11** and **1** ($n = 18$).

containing bilayers give large spectral shifts caused by relative orientation and stacking of the azobenzene units (see Section 3.2). A 1:10 mixed dispersion of azobenzene-containing amphiphile **11** and dialkyldimethylammonium amphiphile **1** ($n = 18$) shows λ_{max} at 355 nm in the high-temperature region, indicating the presence of the isolated azobenzene species. By lowering the temperature, a new peak due to formation of the clustered azobenzene component appears at 315 nm. The spectral change corresponds to the phase transition of the matrix bilayer. This property has been exploited in novel applications of bilayers such as detection of chemical signals[39] and control of chemical reactions.[40]

The limited miscibility of hydrocarbons and fluorocarbons is used for controlled formation of separate domains, as will be discussed in Section 5.

2.4. Bilayer Morphology

Bilayer membranes dispersed in water give in many cases vesicular and lamellar morphologies. Unusual morphologies like the paired leaflet of Figure 5 are also noted. Nonbilayer aggregates have been described for phospholipids.[41] Similarly, Murakami et al. reported that there were interconversions between bilayer and nonbilayer morphologies.[42, 43] In contrast to the charged lipids **12** and **13**, which form typical vesicles and lamellae, their nonionic counterpart **14** is dispersed as nonlamellar network aggregates in the neutral pH range (Fig. 10), but is transformed into multilamellar vesicles in the deprotonated form. Addition of cationic **12** also transforms the nonlamellar aggregate into vesicles. An equimolar mixture of the cationic and anionic amphiphiles leads to nonlamellar networks with repeating distances of 70 and 130 Å in the liquid crystalline temperature region. Small-angle X-ray diffraction suggested the formation of a face-centered cubic lattice.[44]

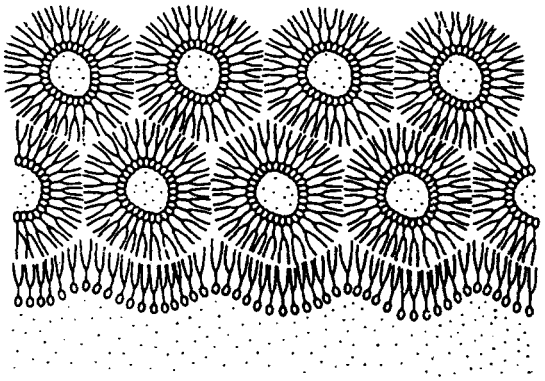

Fig. 10. Nonlamellar network aggregates of the neutral form of **14** [43].

Dynamic morphological changes are intrinsic to many physiological functions of the biological cell. The corresponding study on synthetic bilayer membranes is limited. Rupert et al. examined the ability of vesicles of **1** ($n = 12$) to undergo fusion.[45, 46] They found that dianions such as dipicolinate promoted fusion of vesicles with a diameter of at least 3000 Å, whereas smaller vesicles did not readily fuse despite their aggregation. The fusion was facile when the vesicles were in an overall fluid state. This research group also showed that the lamellar to hexagonal II phase transition proceeded by Ca^{2+}-induced fusion of didodecyl phosphate vesicles.[47] Salt-induced aggregation of dimethyldioctadecylammonium chloride and sodium dihexadecyl phosphate vesicles has been discussed by Carmina-Ribeiro and Chaimovitch.[48]

Optical microscopy is convenient for real-time observation of the morphology change. Evans et al. used video-enhanced contrast-differential interference contrast microscopy to observe dynamic changes of aggregate morphologies of simple double-chain ammonium amphiphiles (**1**, $n = 12$).[49] H. Hotani showed a few years ago that dark-field optical microscopy was particularly advantageous for studying the finer details of biological structures.[50] These investigations confirmed that several transformation pathways existed for various morphologies of liposomes: biconcave, elliptical, regular polygonal, etc.

We applied this technique to examine the morphology of **1** ($n = 12$).[51] The dynamic changes observed are remarkably similar to those of the phospholipids mentioned above. For example, a tubule attached to a vesicle is elongated with time while the vesicle shrinks (Fig. 11 a). A vesicle with protuberance, is converted into a spherical vesicle via an irregular intermediate (Fig. 11 b), and a tadpole and a tripod interconvert (Fig. 11 c). Electron microscopy of freeze-fracture replicas of this dispersion shows that elongated tubules branch

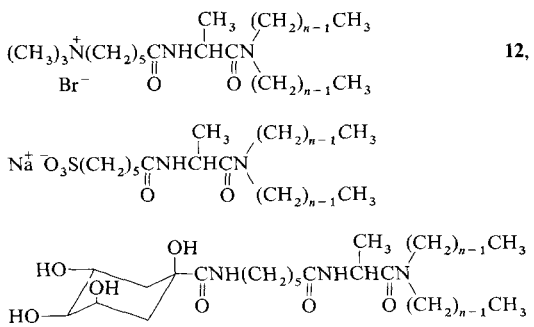

12, $n = 12, 14, 16$

13, $n = 14, 16$

14, $n = 14, 16$

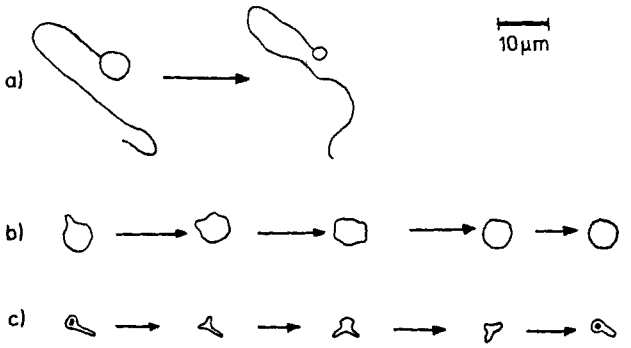

Fig. 11. Schematic illustration of morphological transformation of an aqueous dispersion of **1** ($n = 12$).

into smaller tubules and fibers, which, in turn, are transformed into trains of very small vesicles (diameter, 300–400 Å). The dark-field optical microscopy was further em-

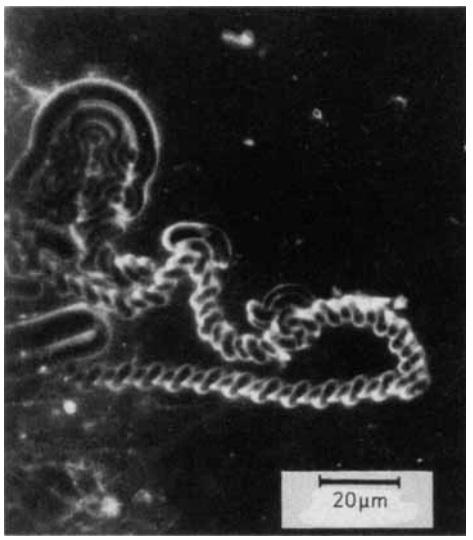

Fig. 12. Dark-field optical micrograph of an aqueous dispersion of **15** ($n = 2$).

ployed for observation of Myelin figures and double-helical fibers of bilayers of double-chain ammonium amphiphile **15** (Fig. 12)[52] The latter morphology was observed for egg-yolk lecithin.

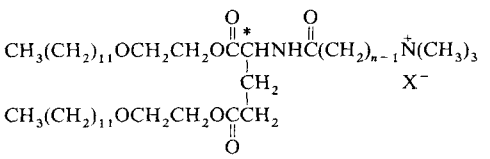

15, $n = 2$ (X = Cl), 11 (X = Br)

3. Bilayer Membranes of Single-Chain Amphiphiles

3.1. Molecular Design

Attachment of two alkyl chains, instead of one, to a single head group should enhance molcular orientation in aggregates because their conformational mobility is restricted. The larger liquid crystalline region in the phase diagram of double-chain amphiphiles compared with that of single-chain counterparts is consistent with this view. If this were the case, stable bilayer membranes would be produced even from single-chain amphiphiles whose conformations are restricted by incorporation of rigid segments or by intermolecular interactions.

Figure 13 illustrates a design principle of a bilayer-forming, single-chain amphiphile. A conventional liquid crys-

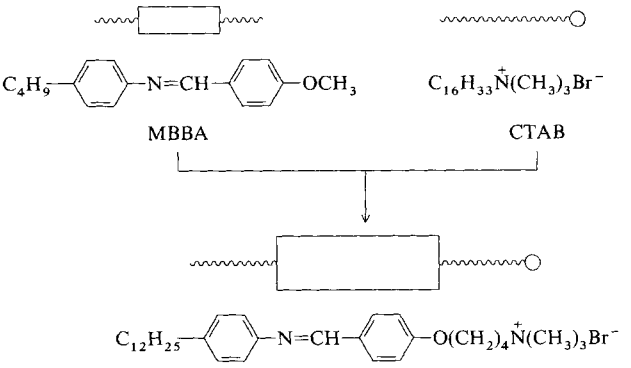

Fig. 13. Design of a single-chain bilayer component by combining the structural features of a compound capable of a liquid crystal transition (MBBA) and a tenside (CTAB).

talline material, MBBA, contains a rigid Schiff base unit connected to a flexible alkyl chain. A micelle-forming surfactant, CTAB, contains a trimethylammonium head group and a hexadecyl chain. The combination of the structural features of these two compounds results in a novel amphiphile that should form aqueous aggregates with a molecular orientation better than that of the conventional micelle. It contains a hydrophilic head, a spacer, a rigid segment, and a flexible tail as structural modules.

Within this structural framework (as in **16** and **17**), the lengths of the methylene chain of the spacer and of the hydrocarbon tails were varied, and their aggregation behavior examined (Table 4).[53] Molecular aggregation detected by

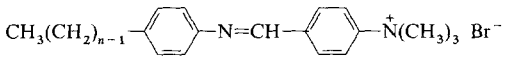

16, $n = 0, 4, 7, 12$

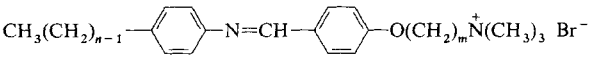

17, $n = 0, 4, 7, 12$, $m = 4, 10$

surface tension measurements occurs at concentrations of 10^{-4}–10^{-5} M except for **16** ($n = 0$) and **17**(0, 10), which did not show any appreciable lowering of surface tension. The critical aggregate concentration is lowered by lengthening of the hydrocarbon tail (C_n portion), but is affected little by the length of the intervening methylene group (C_m portion). The critical aggregate concentrations for **16** ($n = 4$) and **17** (4, 10) lie in the common range of $(2-3) \times 10^{-4}$ M. The critical

aggregate concentration for **16** ($n = 12$) contrasts sharply with that of **17** (0, 10) or **17** (4, 10). In terms of the hydrophile–lipophile balance, these compounds should show similar results. Since this is not so, the location of the rigid segment must determine, to a large extent, the tendency of these amphiphiles to align at the air–water interface.

Table 4. Aggregate behavior of single-chain amphiphiles.

Amphiphile	n	m	cmc [a] [mM]	M [b]	Electron Micrograph
	0		>10	$<10^4$	unstructured
16	4		0.22	1×10^5	unstructured
	7		0.06	8×10^6	lamella
	12		0.01	4×10^6	vesicle and lamella
	4,	4	0.16	8×10^6	unstructured
	7,	4	0.01	2×10^7	lamella
	12,	4	0.01	4×10^6	vesicle
17	0,	10	>10	4×10^6	unstructured
	4,	10	0.33	6×10^6	unstructured
	7,	10	0.02	2×10^7	vesicle
	12,	10	0.01	1×10^7	lamella

[a] Critical aggregate concentration. [b] Molecular weight determined by light scattering.

The average molecular weight of most of the aggregates is 10^6–10^7. Therefore, the average aggregation numbers are in the range of 10^3–10^5. The electron microscopic observation establishes the structural requirement for the formation of a stable bilayer. The development of the bilayer structure is improved with increasing chain lengths of the flexible tail (C_n portion), the minimal chain length being probably between $n = 7$ and $n = 4$. It is worthy of emphasis that **16** ($n = 4$) and **17** (4, 10) fail to form well-organized assemblies in spite of their formation of very large aggregates. A certain tail length is required for an amphiphile to align in aqueous aggregates as well as at the air-water interface.

A systematic variation of lengths of flexible tail and spacer was also conducted for azobenzene-containing, single-chain amphiphiles **18**.[54] Among the total of 21 compounds, the

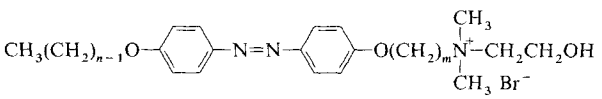

18

formation of stable bilayer membranes as judged by three criteria was concluded for the following combinations of tail length n and spacer length m: $n = 12/m = 2$–$12/n = 10$, $m = 5$–$10/n = 8$, $m = 10$. These results indicate that the tail length is more critical than the spacer length in bilayer formation.

The subsequent studies on molecular design of the single-chain amphiphile established that the kind of head group could be varied as much as those of the double-chain counterpart (cationic, anionic, nonionic, and zwitterionic)[55, 56] and that the rigid segment is extensively variable[57, 58] (Scheme 2). An extensive list of this class of single-chain compounds was compiled.[59] Cho et al. recently reported that an ammonium derivative of cholesterol formed bilayer

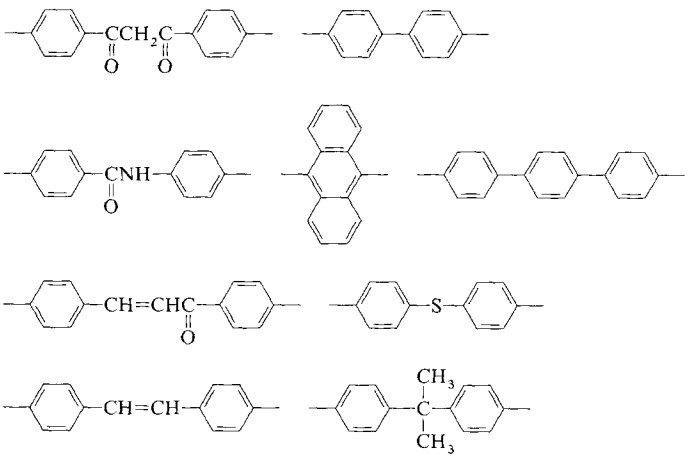

Scheme 2. Examples of rigid segments for single-chain bilayer-forming amphiphiles. For more examples see Scheme 3.

vesicles.[60] It has to be noted that „the rigid segment" implies the structural unit which promotes molecular alignment by intermolecular stacking and other intermolecular interactions. The aromatic „rigid segment" of Scheme 2 promotes intermolecular stacking. The molecular alignment can be improved in single-chain ammonium amphiphiles by strong hydrogen-bonding capability.[61]

3.2. Molecular Orientation within the Bilayer

A systematic structural variation of single-chain amphiphiles indicated that a certain length of the flexible tail was required for bilayer formation. The role of the spacer methylene chain, in contrast, was not clear. The crucial influence of the spacer length on bilayer assembly was first clarified in relation to absorption spectra of the azobenzene bilayer of **18**. Figure 14 shows representative spectral variations which depend on the molecular structure. All the bi-

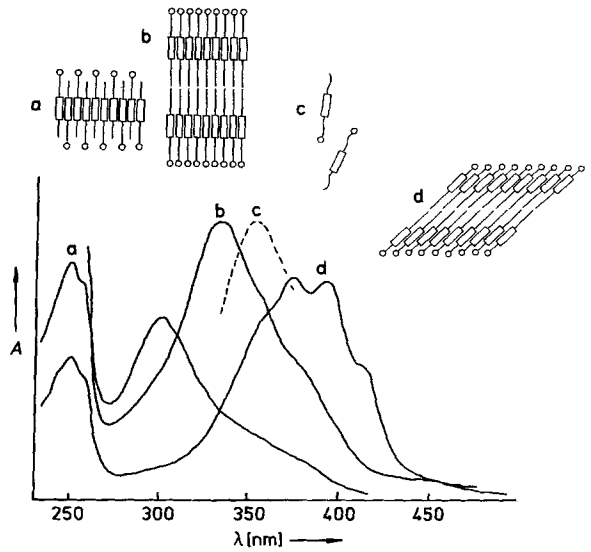

Fig. 14. Absorption spectra and the packing modes of bilayers of **18** (n, m). a) $n = 8$, $m = 10$; H-aggregate; b) $n = 12$, $m = 10$; c) absorption of monomeric azobenzene derivatives; d) $n = 12$, $m = 5$, J-aggregate.

layer components contain the identical azobenzene chromophore, yet their spectral patterns are quite different. λ_{max} covers a wide range from 300 nm for **18** (8, 10) to 390 nm for **18** (12, 5). The observed λ_{max} variation needs to be explained in terms of the chromophore interaction (orientation and aggregation) in the aggregate. According to the molecular exciton model of Kasha,[62] the blue shift for the bilayer of **18** (8, 10) relative to the absorption of the isolated chromophore (λ_{max} 355 nm) results from a parallel orientation of the neighboring transition dipoles (the H-aggregate, Fig. 14a), and a red shift for the bilayer of **18** (12, 5) is attributable to the tilted chromophore orientation (the *J*-like aggregate, Fig. 14d). The other bilayers of **18** (10, 4), **18** (12, 10), and **18** (12, 6) apparently have intermediate orientations (Fig. 14b).

The interdigitated bilayer structure was first proposed for the bilayer of **18** (8, 10) on inspection of the X-ray diffraction of its cast multibilayer film.[63] More recently, Okuyama and co-workers determined its structure from a single crystal (Fig.15).[64] The parallel azobenzene packing is appropriate

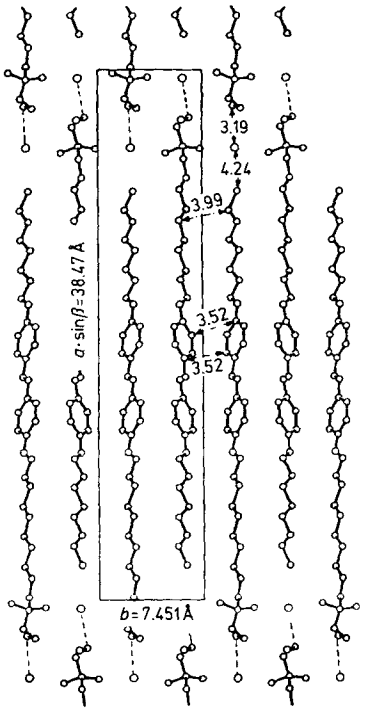

Fig. 15. The packing structure of a single crystal of **18** (8, 10).

for its particular molecular structure, since the cross section of the ammonium head group is about twice the cross section of the hydrophobic portion and the lengths of spacer and tail are very similar.

The crystal structure of the bilayer of **18** (12, 5) is shown in Figure 16.[65] A typical bilayer structure is formed. The tilt angle of the molecular axis from the layer normal amounts to 62°. This inclination is required in the bilayer assemblage in order to match the cross sections of the head group and the hydrophobic chain. The J-aggregate formation inferred from the spectroscopic data is consistent with the crystal structure. The spacer length of $m = 5$ appears essential for the tilted packing, because analogous tilted arrangements are observed for the bilayers with the common $m = 5$ spacer and different tail lengths of $n = 6$, 8, and 10.[66, 67]

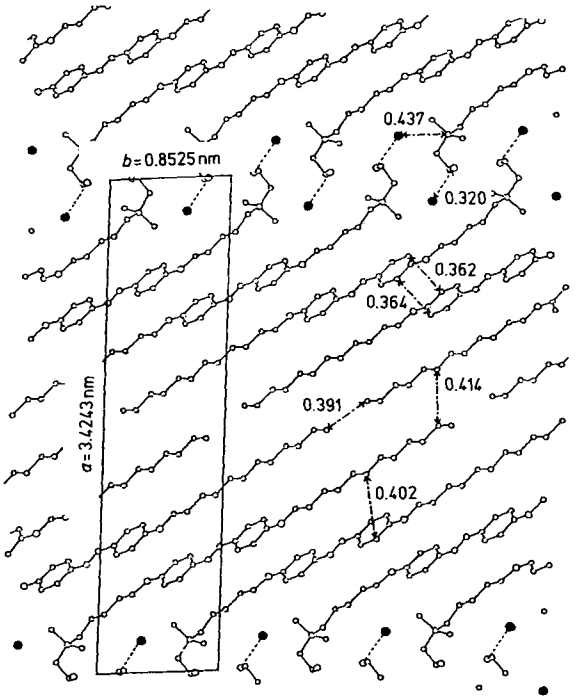

Fig. 16. The packing structure of a single crystal of **18** (12, 5).

X-ray photoelectron spectroscopy (XPS) is also useful for estimation of the molecular packing in single crystals. Nakayama et al.[68] examined the N_{1S} spectrum of a single crystal of **18** (12, 5). The calculated intensity ratio of the azobenzene nitrogen center to the ammonium nitrogen center agreed with the experimental pattern if the molecular axis was assumed to incline ca. 60° to the bilayer normal at the outermost surface of the crystal. This inclination is in close agreement with that determined by X-ray diffraction.

The variation of the molecular alignment with methylene chain lengths is not restricted to bilayers of azobenzene derivatives. Partially interdigitated structures were proposed for **16** ($n = 10$, 12, 14).[69] We very recently prepared a series of single-chain amphiphiles **19** which contain the σ-hydroxydiphenylazomethine unit as rigid segment.[70] The spectral shifts in the absorption spectrum and the layer thickness

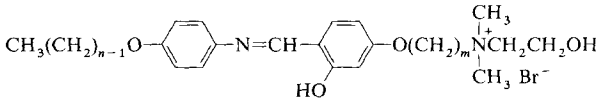

19:(n, m) = (8, 10), (12, 5), (12, 10)

determined by X-ray diffraction of cast films indicated that the effect of alkyl chain lengths on the molecular packing is virtually identical with those of the azobenzene-containing bilayer.

3.3. Morphology of Bilayers

Single-chain amphiphiles form bilayer vesicles and lamellae, similar to those of double-chain amphiphiles. The rigid segment in these amphiphiles promotes regular molecular orientation. The effect of the chemical structure of the rigid segment on aggregate morphologies has been studied systematically for a series of single-chain ammonium amphiphiles.[57] Electron microscopy indicates the formation of aqueous aggregates with various morphologies: the representative cases are globule, vesicle, lamella, rod, tube, and disk (Fig. 17). These morphologies can be explained as arising from different characteristics of the rigid segment, as summarized in Scheme 3. When the rigid segment is biphenyl or azobenzene, globular aggregates (probably collections of small bilayer fragments) are formed. The diphenylazomethine group is structurally similar to the azobenzene group, but their behavior as rigid segment is quite different. The amphiphile with a diphenylazomethine rigid segment produces much better developed bilayer membranes as a result of the dipolar interaction between the diphenylazomethine groups. In the case of the symmetrical rigid segments (biphenyl and azobenzene), the extensive organization appears less favored.

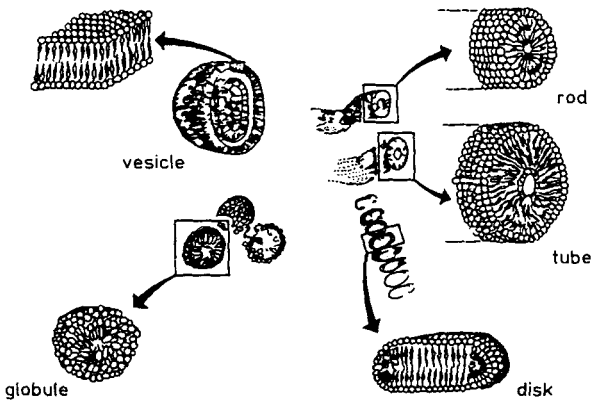

Fig. 17. Aggregate morphologies of single-chain amphiphiles.

A structural feature common to the third group of single-chain ammonium amphiphiles is that they contain bent rigid segments. The bending is either due to single-atom connection of two benzene rings, to rotation of the single bond, or to *meta* substitution. The contrasting behavior of the straight and bent ammonium amphiphiles is interesting. The straight molecules tend to assemble in a neat, two-dimensional arrangement (membrane), but the bent molecules give rise to curvatures which result in a radial molecular arrangement (rodlike and tubular structures). Double *meta* substitution at the rigid segment produces less organized aggregates.

The disk structure contains two kinds of molecular arrangement. One is the two-dimensional arrangement (flat portion) as in the typical bilayer membrane, and the other is a highly curved arrangement (side of the disk) as in the rodlike structure. The fourth group of amphiphiles can assume both the extended and bent conformations, which may be used advantageously to produce the two kinds of molecular packing involved in a disk.

These morphological correlations suggest that the surface curvature of an aggregate is controlled by appropriate mixing of different classes of amphiphiles. Amphiphile **17** (12, 4) gives well-developed, multilamellar vesicles (Fig. 18a). Replacement of this rigid segment with the diphenyl ether unit results in a tubular morphology (Fig. 18b). A 1:1 mixture of

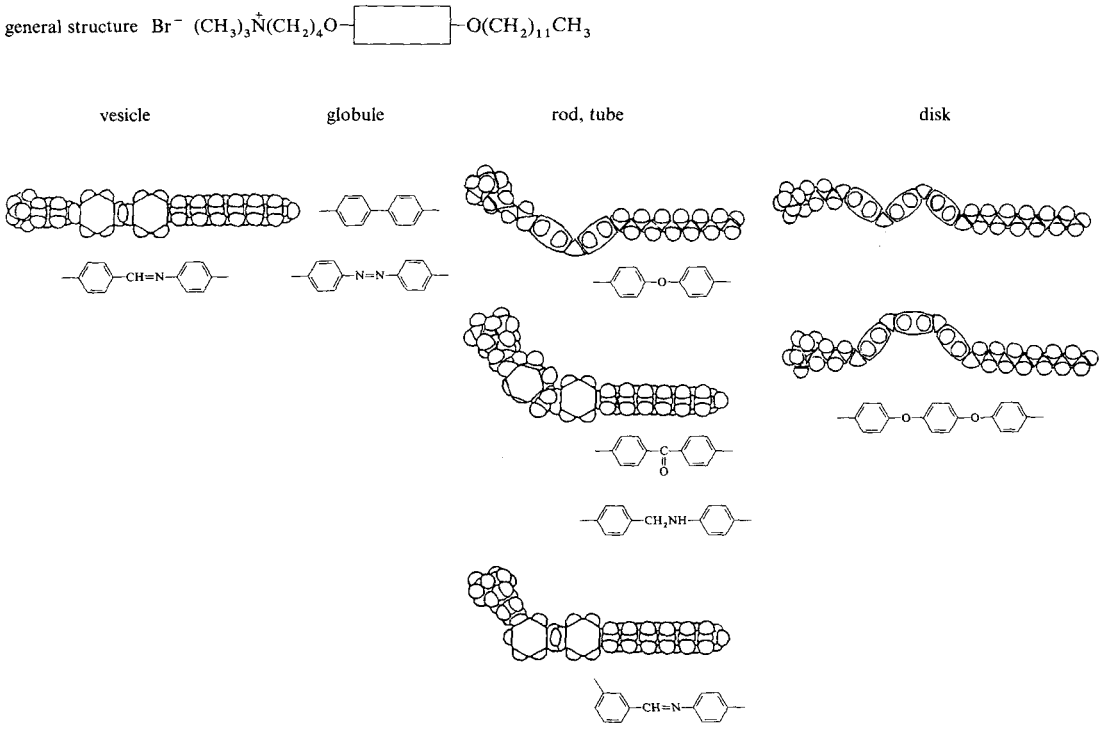

Scheme 3. Schematic representation of the morphology of aggregates and the rigid segments which gives rise to them.

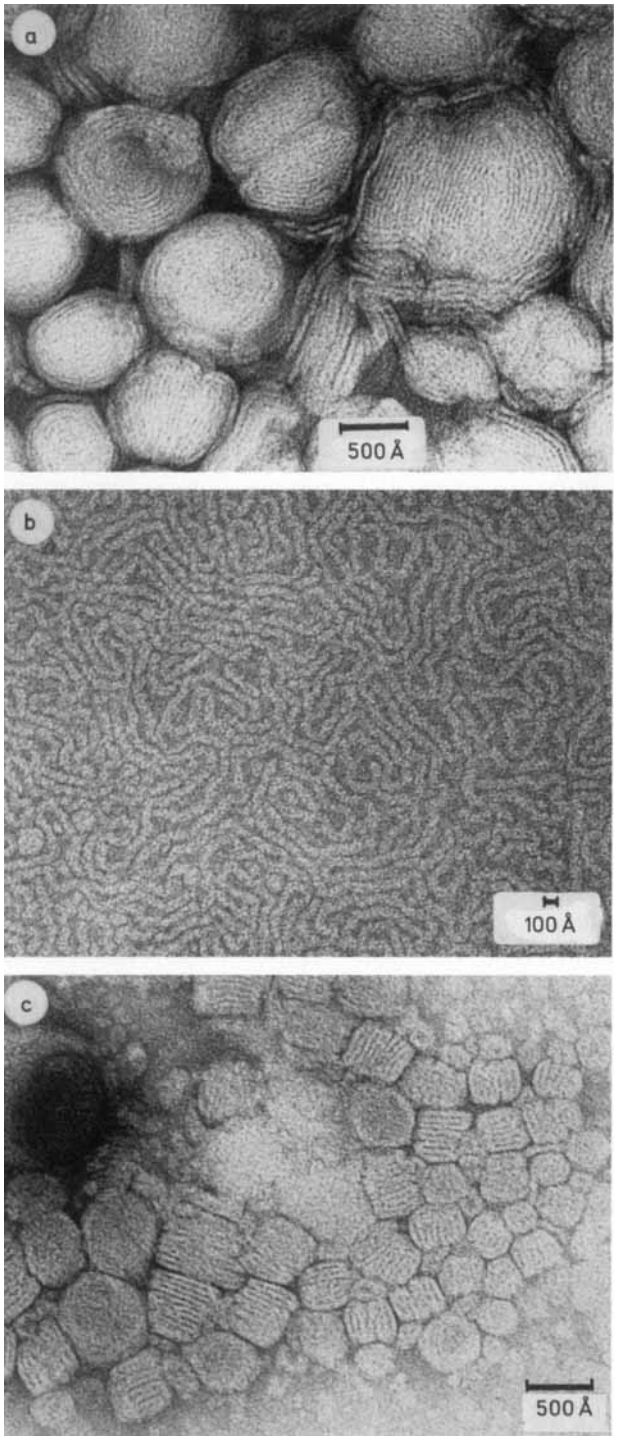

Fig. 18. Electron micrographs of aqueous bilayer dispersions of single-chain ammonium amphiphiles (negatively stained by UO_2^{2+}). a) **17** (12, 4); b) **20**; c) a 9:1 mixture of **17** (12, 4) and **20**.

these amphiphiles gives tubular aggregates very similar to Figure 18b. When the molar ratio is 7:3, an obscure mixture of tubes and lamellae is found. A 9:1 mixture produces stacked disks (or stacked patches of bilayers) with a layer thickness of 40–50 Å (Fig. 18c). It is conceivable that the flat portion of the disk is mainly composed of **17** (12, 4), and that **20** is concentrated along the side of the disk where large curvature is required.

A related morphology control is found for a mixture of **17** (12, 4), and **21**. Cosonication of multiwalled vesicles of **17** (12, 4) and globular **21** gives single-walled vesicles.

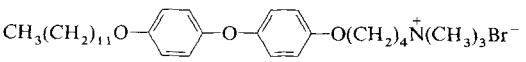

20

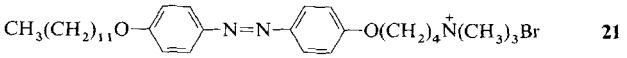

21

4. Molecular Membranes of Multichain and Two-Headed Amphiphiles

4.1. Triple-Chain Amphiphiles

As discussed in Section 1, the hydrophile–lipophile balance is not the most crucial factor that determines bilayer formation. Certain degrees of imbalance will be accommodated by the stabilization gained by molecular alignment. Compounds **22**–**24** are examples of triple-chain ammonium amphiphiles that were tested for bilayer formation.[71]

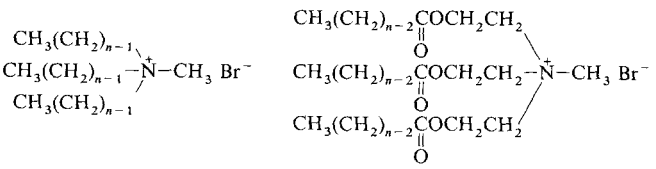

22, $n = 12, 16$ **23**, $n = 12, 16$

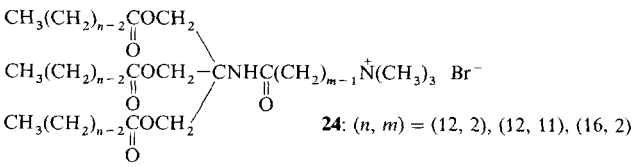

24: $(n, m) = (12, 2), (12, 11), (16, 2)$

Simple triple-chain compounds **22** do not seem to give well-developed bilayer structures. Amphiphiles **23** and **24** form stable bilayer membranes in water, as inferred from their huge molecular weights, the presence of a phase transition, and electron microscopic observation. The CPK molecular

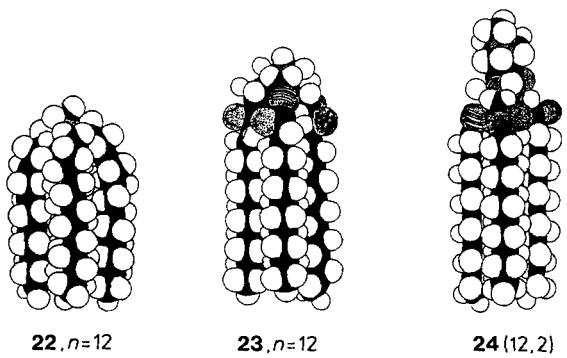

Fig. 19. CPK model of triple-chain amphiphiles with different connectors. The parallel alignment of the alkyl chains in **22** is inferior to that in **23** and **24**.

models of these amphiphiles with different connector structures (Fig. 19) endorse these experimental observations. In the case of **22** ($n = 12$), the long alkyl chains cannot be aligned at locations close to the ammonium group because of its tetrahedral configuration. In contrast, the alkyl chains of **23** ($n = 12$) can be well aligned. The compact chain packing is produced by the presence of the ester unit, and the ammonium head can protrude without conformational constraint. The same situation is found for **24** (12, 2), again due to the presence of the ester linkage.

4.2. Quadruple-Chain Amphiphiles

Very recently, we discovered that even quadruple-chain ammonium amphiphiles such as **25** are suitable for two-dimensional molecular alignment.[72] These compounds give

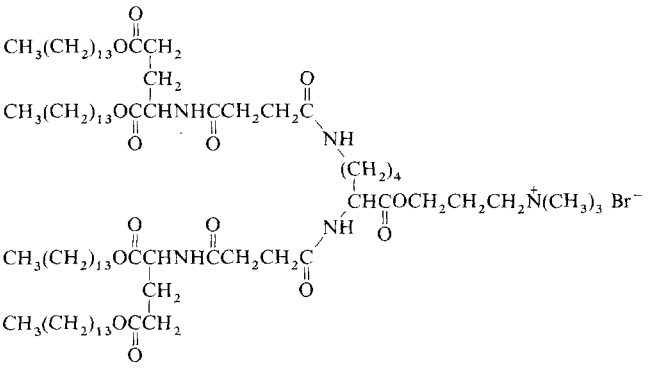

25

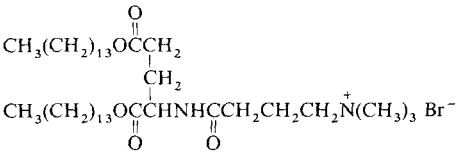

26

transparent aqueous dispersions at 20 mM, and display typical bilayer characteristics. Electron microscopy indicates the formation of vesicles and tapelike aggregates. A DSC experiment showed the presence of the phase transition peak. The transition behavior of **25** is not very different from that of the corresponding double-chain amphiphile **26**. The chain alignment is strongly dependent on the kind of the connector. The chiral unit in **25** and **26** should produce different chiral binding sites at the membrane surface.

The native counterpart of these amphiphiles is four-chained cardiolipin. It is interesting to note, however, that cardiolipin cannot form a stable bilayer assembly by itself.

4.3. Two-Headed Ammonium Amphiphiles

Some archeobacteria contain another class of membrane lipids. One of those lipid components is a macrocyclic amphiphile that spans the bilayer thickness.[73] Covalent bonding of alkyl chain ends of synthetic bilayer components would produce two-headed amphiphiles which may form monolayer membranes in water.

Structural extention of single-chain, bilayer-forming amphiphiles to two-headed amphiphiles results in molecular structures such as **27**–**29**.[74] Two ammonium groups at the ends of a molecule are connected by a single chain that is composed of methylene chains and aromatic unit. They are all dispersed in water as stable aggregates with molecular weights of 10^6–10^7. Electron microscopy shows that lamellae and rodlike structures are formed. As shown in Figure 20, **27** (10 mM) gives highly developed lamellae with layer thickness of 30–40 Å. This figure corresponds to the extended molecular length; therefore, the bisammonium molecule is aligned normal to the layer plane. Molecular elongation and increase in the flexible hydrocarbon chain as in **28** (molecular length, 67 Å) leads to the appearance of tubular structures (diameter 70–100 Å), with dark striations (deposits of uranyl acetate) in the middle. The flexible methylene chain in the center of the molecule would allow the bent molecular packing required for the tubular morphology (Fig. 20b).

The rigid lamella of Figure 20a can be transformed into single-walled vesicles as in Figure 20c by cosonication with cholesterol in the ratio 3:1. The vesicles are 1000–3000 Å in diameter and 60–70 Å in layer thickness. We propose that cholesterol molecules are preferentially located in the outer half of the membrane, thus creating surface curvature suitable for vesicle formation (see Fig. 21a). Remarkable transformations of morphology of lecithin vesicles by addition of lysolecithin and cholesterol were reported in a landmark paper of Bangham and Horne in 1964.[1]

Another way of creating curvature is the use of unsymmetrical bisammonium compounds. Attachment of a decyl chain to one of the ammonium heads of **27** changes the aggregate morphology from lamella to multiwalled ves-

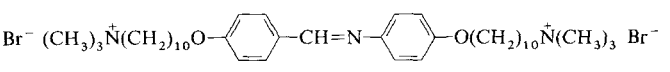

27

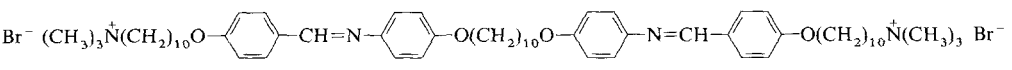

28

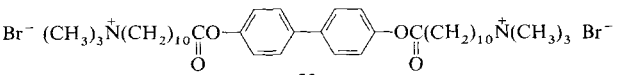

29

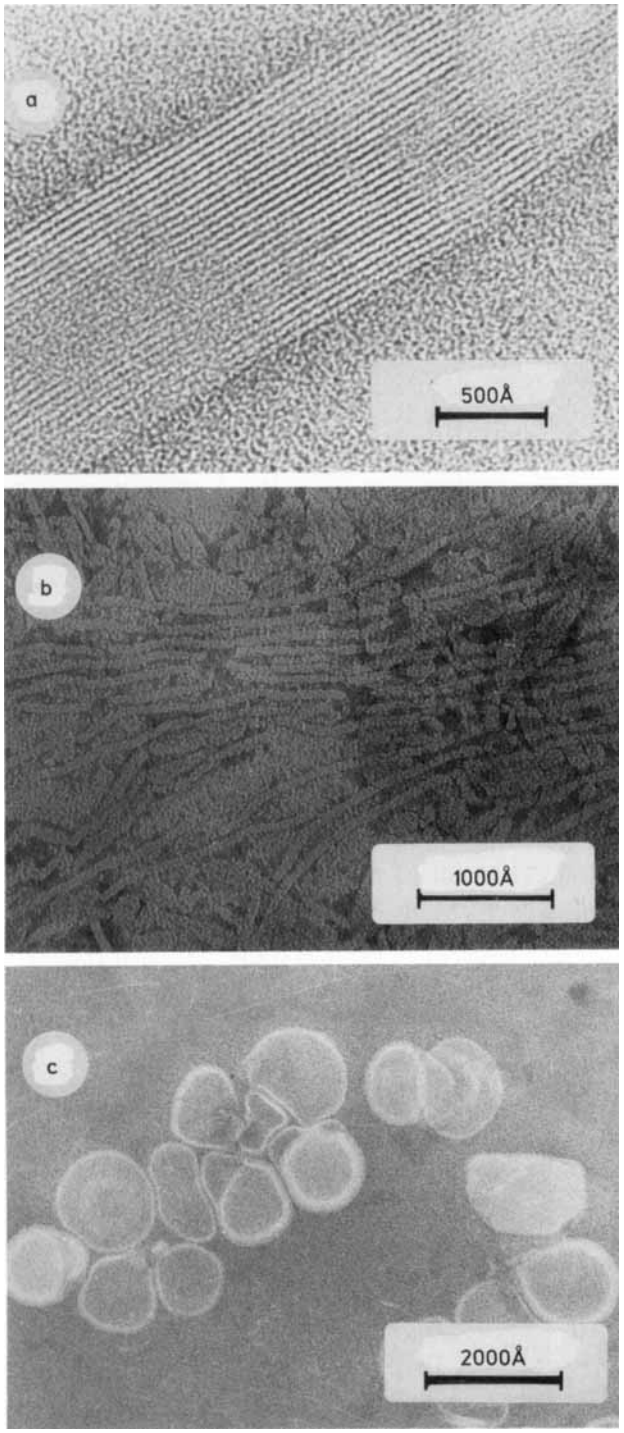

Fig. 20. Electron micrographs of aqueous dispersions of two-headed ammonium amphiphiles (stained by UO_2^{2+}). a) **27**; b) **28**; c) **27** + 1/3 cholesterol.

icles.[75] The decyl-substituted ammonium head in **30** seems to be more populous in the outer surface (Fig. 21 b).

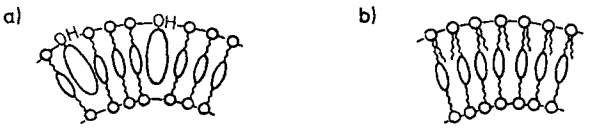

Fig. 21. Creation of surface curvatures in monolayer membranes. a) **27** + 1/3 cholesterol; b) **30**.

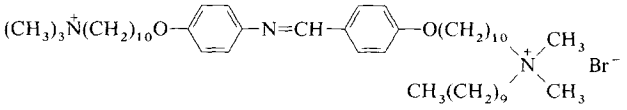

30

Formation of monolayer vesicles was reported by Fuhrhop and co-workers from single-chain amphiphiles with two viologen head groups (**31**).[76] They subsequently

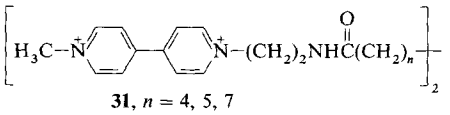

31, $n = 4, 5, 7$

conducted extensive research on this type of compounds, the bolaamphiphiles. For example, they prepared a series of macrocyclic compounds with two polar head groups and studied their vesicle formation.[77]

Amphiphiles related to **27**–**31** can be designed by combining only one end of the alkyl chain in double-chain amphiphiles.[78] Bisammonium compound **32** and related ionene oligomers **33** can form monolayer membranes.

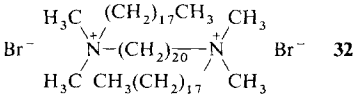

32

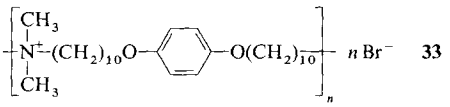

33

5. Bilayer Membranes of Fluorocarbon Amphiphiles

A new class of bilayer membranes are derived by replacement of hydrocarbon chains with fluorocarbon chains. They are single-, double-, and triple-chain compounds; for example, **34**–**38**.[79–82]

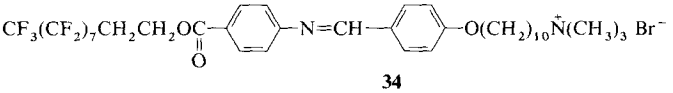

34

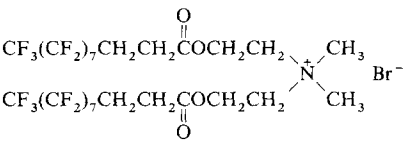

35

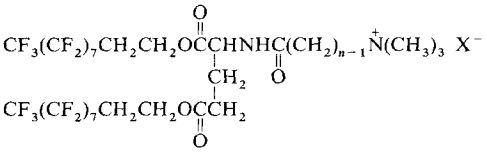

36, $n = 2-11$, X = Cl, Br

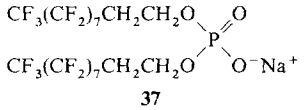

37

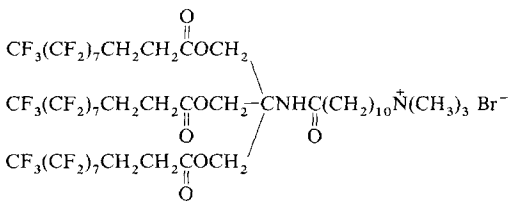

38

Sonication of these amphiphiles in water produces clear to translucent dispersions. Electron microscopic observation after the negative staining reveals the existence of the bilayer structure (vesicles and/or lamellae). For instance, **35** gives well-dispersed, single-walled vesicles. A related hydrocarbon (dodecanoate) amphiphile produces multi-walled vesicles. Double-chain **39**, which possesses both fluorocarbon and hydrocarbon tails gives even better developed single-

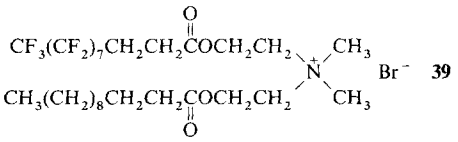

39

walled vesicles. Those amphiphiles which differ only in the tail portion (fluorocarbon vs. hydrocarbon) show aggregation morphologies that are fairly similar. Single-chain amphiphile **34** and triple-chain amphiphiles like **38** also produce bilayer aggregates.

Fluorocarbon bilayers exhibit small endothermic peaks in DSC thermograms. The phase transition temperature (T_c) of the fluorocarbon bilayers is detected at temperatures 20–30 °C higher and have smaller enthalpy changes than those of hydrocarbon bilayers. The smaller enthalpy changes to be an inherent property of bilayers made from fluorocarbon amphiphiles.

Figure 22 illustrates, as an example, the variation of fluorescence depolarization P of diphenylhexatriene embedded in bilayer membranes of the triple-chain amphiphiles.[82] At low temperatures, the P values are large irrespective of the number of fluorocarbon chains, but they decrease sharply near T_c, leading to large P differences. These data indicate that 1) the membranes are equally rigid at low temperatures, 2) the fluidity increases (decrease in P) at the temperature regions which correspond to the respective DSC peaks, and 3) the membrane fluidity of the liquid crystalline bilayer (at $T > T_c$) decreases with increasing number of fluorocarbon chains.

Fluorocarbons are not readily miscible with the corresponding hydrocarbon compounds. This is exemplified by the formation of heterogeneous micelles from fluorocarbon and hydrocarbon surfactants.[83] In the same vein, fluorocarbon and hydrocarbon bilayers show limited miscibilities. This situation can be improved by adding unsymmetrical components such as **39**. The improved miscibility is also

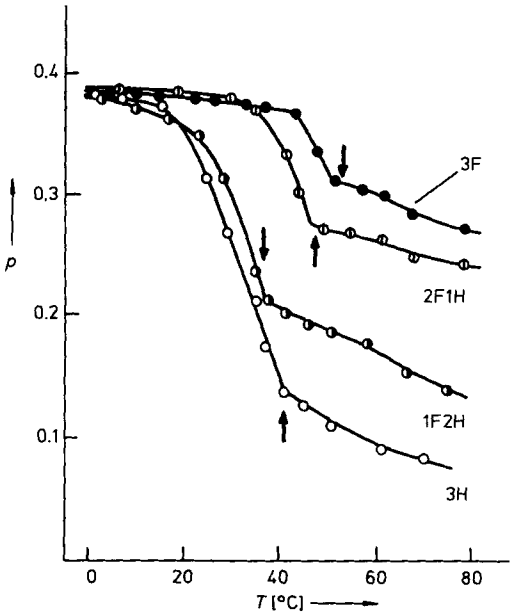

Fig. 22. Fluidity of fluorocarbon bilayers, measured by fluorescence depolarization P of diphenylhexatriene embedded in them. The arrows indicate the T_c values determined by DSC. 3F = **38**, 3H = **24** (12, 11); in 2F1H one and in 1F2H two fluorohydrocarbon chains of **38** are replaced by hydrocarbon chains of **24** (12, 11).

demonstrated in the case of triple-chain bilayer components. As shown schematically in Figure 23, the hydrocarbon component (3H) and the fluorocarbon component (3F) are hardly miscible. Upon addition of a partially fluorocarbon-

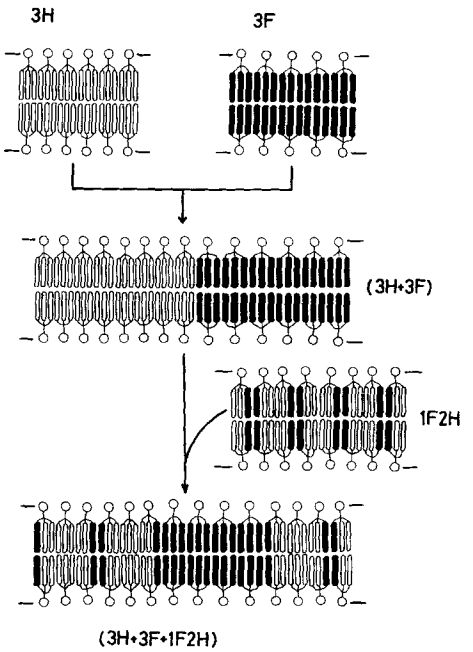

Fig. 23. Miscibility of bilayer membranes of triple-chain amphiphiles containing fluorohydrocarbon and hydrocarbon chains, before and after addition of a mixed amphiphile.

tailed amphiphile 1F2H, the original two components become more miscible.

General aggregation behavior of the fluorocarbon amphiphiles is closely related to that of the corresponding hy-

drocarbon compounds. However, the bilayer properties are very different for the two systems: First, fluorocarbon bilayers are much less permeable than hydrocarbon bilayers toward ions and small molecules. Second, these two membrane components tend to form separate domains, and the phase separation has been effectively used for controlled permeation and catalysis.[81]

6. Chiral Bilayer Membranes

As discussed in Section 2, the amino acid unit acts as a useful module in the design of bilayer-forming compounds. Some of the resulting chiral bilayers of single-chain and double-chain amphiphiles display much enhanced circular dichroism (CD).[84, 85] These data suggested that the chiral components were arranged asymmetrically in fixed spatial dispositions as a result of the formation of higher order structures.

A fairly simple, double-chain amphiphile, L-**40** forms single- and double-walled vesicles with diameters of 300–1000 Å, when dispersed in water by sonication (Fig. 24a).[86]

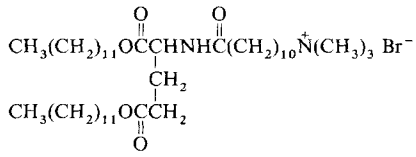

40

These vesicles are slowly transformed into the helical morphology which is made of twisted tapes, as shown in Fig. 24b). Further ageing gives tubes with helical streaks. These helices and tubes are better observed by dark-field optical microscopy (Fig. 24c)[87] and by high-resolution scanning electron microscopy (Fig. 24d).[88] An advantage

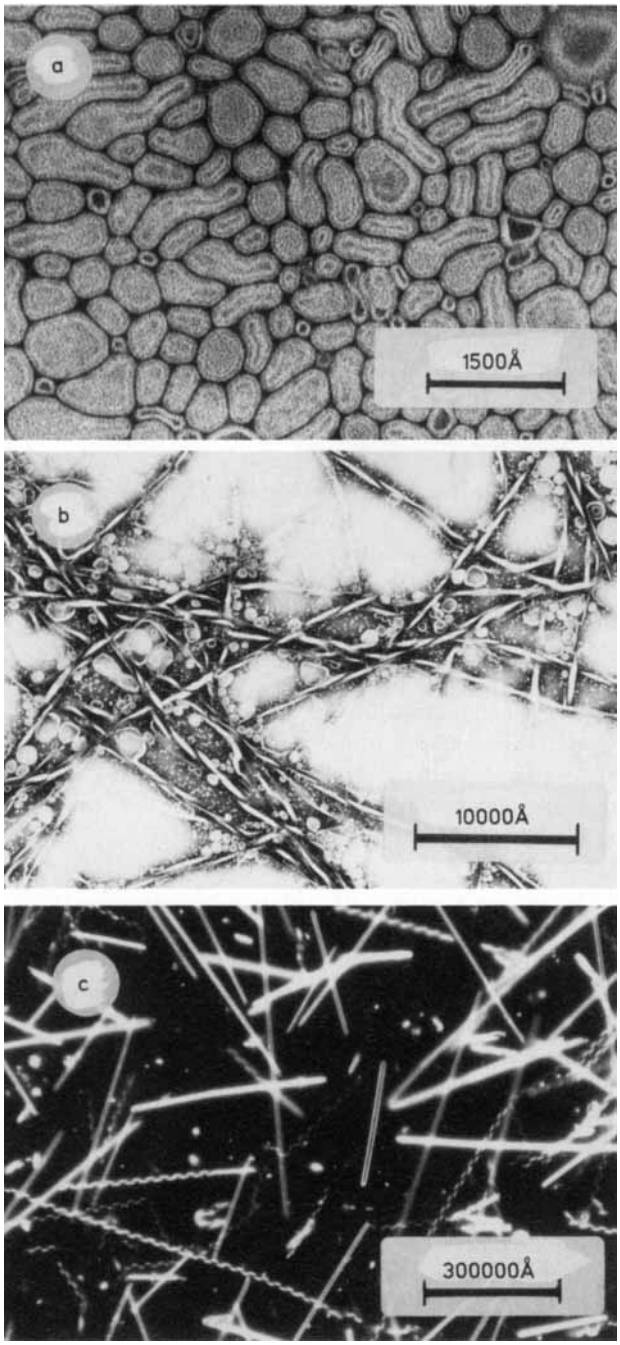

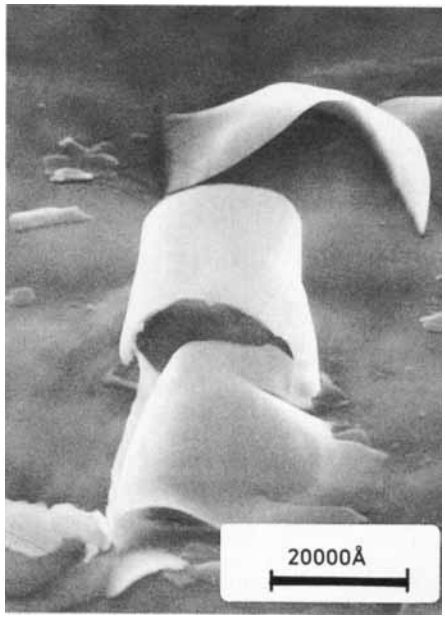

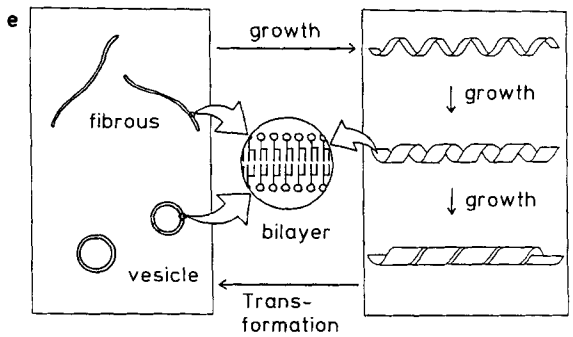

Fig. 24. Formation of helical superstructures from bilayer membranes of chiral ammonium amphiphiles. a) Electron micrograph of aqueous vesicles of L-**40**; no ageing, stained with UO_2^{2+}. b) Electron micrograph of the helical superstructure of L-**40**; stained by UO_2^{2+}. c) Dark-field optical micrograph of the helical superstructure of L-**40**. d) Electron micrograph (high resolution scanning electron microscopy) of the helical superstructure of L-**40**. e) A schematic illustration of helix formation.

of the latter two microscopic methods is that direct images are obtainable. The growth and degradation processes of the helices in water is observable by optical microscopy at a resolution of 1 μm, and the three-dimensional structure of the molecular aggregate can be determined by the scanning electron microscope at a theoretical resolution of less than 10 Å.

The helical superstructure is maintained only in the crystalline state. When the aqueous dispersion of L-**40** (T_c of the bilayer, 33 °C) is warmed to 35 °C, the helices and tubes are all converted into large flexible vesicles. The melting process can be observed directly by optical microscopy.

Enantiomeric amphiphile D-**40** similarly showed a slow growth of helices. These are left-handed, in contrast to the right-handed helices of the L enantiomer. In the case of its racemic bilayer, initially formed vesicles are converted into rodlike aggregates without formation of helices.

Helix formation is sensitive to the molecular structure. It is not observed for a closely related amphiphile with a shorter spacer length: CH_2 instead of $(CH_2)_{10}$. The shorter spacer may interfere with the regular molecular arrangement, since this amphiphile instead forms smooth single-walled vesicles.

The helical superstructure has been obtained for other bilayer-forming amphiphiles. Single-chain ammonium amphiphile **41** gives helical superstructures accompanied by CD enhancement.[89] Cho and Park reported helical superstructures formed by cationic cholesterol-containing polymers.[60] Yamada et al.,[90] concurrently with our initial finding, observed that dialkyl amphiphiles with the oligoglutamate head group **42** produced helical superstructures (twisted ribbons with a layer thickness of 30–40 Å). Single- and double-chain phosphate amphiphiles can form helical superstructures as well.[91] Tubular aggregates, which are products of helical growth, are found in a dispersion of a diacetylenic phosphocholine lipid.[92] Related helical fibers of lipid bilayers were obtained from *N*-octylaldonamides.[93, 94]

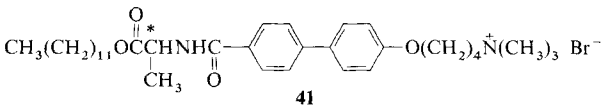

41

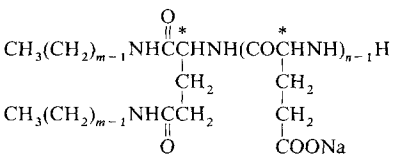

42, $m = 12, 16$

7. Applications and Further Developments

In the preceding sections we described molecular design and basic physicochemical properties of synthetic bilayer membranes. Since a multitude of physiological functions involve biomembranes, functional applications of synthetic bilayers should be numerous. They are briefly described in the following.

7.1. Models and Substitutes of the Biomembrane

The basic structural and physicochemical features of synthetic bilayer membranes are common to those of bilayer membranes of natural lipids. Therefore, lipid components of biological membranes may be replaced with their synthetic counterpart. For example, Ringsdorf and co-workers[95] reconstituted ATPase in a polymerized bilayer membrane of a diacetylenic amphiphile. O'Brien et al.[96] used partially polymerized vesicles of a dienoyl phosphatidylcholine to incorporate rhodopsin without denaturation. We have shown recently that myoglobin, the water-soluble heme protein, can be embedded in the interbilayer region of cast films of synthetic amphiphiles without denaturation.[97] The spatial orientation of myoglobin is fixed apparently by electrostatic attraction between the positively charged residue of the protein surface and the negative phosphate unit of the bilayer membrane. Interestingly, the membrane-bound myoglobin displayed redox reactivity.[98] This functional conversion opens an exciting future for composite molecular systems that are composed of natural and artificial molecules.

Murakami and co-workers recently carried out an extensive investigation on the use of functionalized synthetic bilayers as enzyme-like reaction sites for vitamin B_6-dependent transamination and β-replacement reactions,[99] and vitamin B_{12}-dependent carbon-skeleton rearrangements.[100]

7.2. Substrate Trapping and Reaction Control

Synthetic bilayer vesicles can retain ions and molecules in the inner aqueous phase, just like liposomes of biolipids. In addition, a large number of polymerized synthetic vesicles have been investigated to obtain stabilized drug carriers.[11] The trapping capability leads to separation of chemical species inside and outside the vesicles. This has been studied by many research groups in order to mimic the conversion of solar energy in the photosynthetic reaction center.[101] Other organic reactions were also affected by reactant separation by bilayers and by flip-flop exchanges of reaction bilayer components.[102]

The molecular organization and the physical state (phase separation and phase transition) of bilayers can be used as effective means to control reactions. For instance, phase separation (domain formation) of two reacting species produce a unique feature of reactivity.[40] It is possible to construct a surface receptor which performs discrimination, transduction, and amplification of chemical signals by inducing phase separation.[39]

7.3. Designed Organization of Functional Units

The two-dimensional feature of bilayer membranes is particularly advantageous for designed alignment of photonic, electronic, and magnetic functional units. A correlation be-

tween the chemical structure and the component alignment as discussed in Section 3.2 is useful in this respect. A bilayer of an azobenzene derivative, which possesses a tilted (J-like) molecular packing (see Fig. 14), shows highly efficient electron transfer and energy transfer within the bilayer and to a membrane-bound cyanine dye. These efficient transfers are not observed for analogous bilayers with parallel chromophore stacking.[103]

Some oppositely charged dye molecules are bound to the bilayer surface in a specific manner. For example, anionic cyanine dyes are bound to ammonium bilayer membranes in water either as the monomeric species, as H-aggregates, or as J-like aggregates.[104]

When the polar head of bilayers is a chelating group that binds transition metal ions, electron spins are aligned at the membrane surface. A single-chain amphiphile with the cyclam head group forms a bilayer Cu^{II} chelate, which displays a strong antiparamagnetic interaction.[105] Modifications of the metal complex organization should give rise to interesting magnetic and optical properties.

7.4. Surface Monolayers, Langmuir–Blodgett (LB) Films, and Planar Lipid Membranes (BLM)

Most of the bilayer-forming amphiphiles can form stable monolayers at the air-water interface. That the molecular orientations in monolayers and in the corresponding LB films are closely related to those in aqueous bilayers was demonstrated by absorption spectroscopy.[106] The self-assembling property of these amphiphiles is particularly suitable for enhancing the monolayer stability and the subsequent deposition as LB films. Stable BLMs are also formed from many double-chain ammonium amphiphiles.[107] The extent of alkyl chain alignment critically affects the life time. Common structural features exist for the aggregation behavior of aqueous bilayers, surface monolayers, and BLMs (planar bilayers). Therefore, the molecular design discussed in this article is useful for developing new LB films and BLMs.

7.5. Cast Films and Their Use as Molecular Templates

The outstanding self-assembling property of bilayer membranes is fully demonstrated by the formation of free-standing cast films. Transparent films with regular, multilayer structures are readily obtained when aqueous dispersions of synthetic bilayer membranes are spread on solid supports,[63, 108] as is the case with some phospholipids.[109] It is remarkable that flexible, self-supporting films are obtainable from non-covalent molecular aggregates. Unique molecular sensors and permeation control have been realized by application of these cast films.[110]

The macroscopic anisotropy of the cast film has been used to incorporate planar metal complexes into designed spatial arrangements.[111] More recently, Ishikawa and Kunitake[112] demonstrated that anionic porphyrins are incorporated into cast films of ammonium bilayer membranes in specific spatial orientations, depending on the optimized electrostatic attraction of the negative charge on the porphyrin ring and the positively charged bilayer surface. This methodology should lead to designed molecular systems.

Because of the stability of synthetic bilayers as independent entities, the regular bilayer organization is maintained even when guest molecules are introduced in the interbilayer space of a cast film. Cross-linking of a polymerizable guest and the subsequent removal of the bilayer matrix by solvent extraction produces multilayers of two-dimensional molecular networks.[113, 114] This approach is also applicable to synthesis of molecularly controlled siloxane networks[115, 116] and to the hydrolysis of $FeCl_2$ in a cast film to obtain oriented iron oxide particles.[117] It is clear that cast multibilayer films serve as superb templates for preparation of two-dimensional organic and inorganic materials. Sol–gel condensation of inorganic starting materials in the multibilayer matrix results in novel ceramics with molecular precision.

7.6. Bilayer Assembly in Organic Media

The major driving force of self-assembly of biomembranes and synthetic molecular membranes is the hydrophobic interaction. It is lost in organic solvents with which alkyl tails of the membrane component are miscible. We recently took advantage of the immiscibility of fluoroalkyl chains with conventional organic solvents, in order to prepare bilayer assemblies in organic media.[118, 119] The principle of their molecular design is common to that of aqueous bilayer membranes, although the hydrophilic head group has to be replaced with flexible hydrocarbon groups such as in **43**. Compartmentalization of the molecular space and novel organization of functional molecules are just two examples of the versatile possibilities we can envisage for this system.

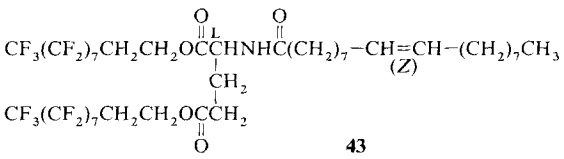

43

Our research described in this review was made possible only through dedication of our co-workers. The author wishes to express his gratitude to these people. He also appreciates the help of Ms. R. Ando, Ms. C. Tsuda, and Mr. T. Nishimi in the preparation of the manuscript.

Received: August 6, 1991 [A 867 IE]
German version: *Angew. Chem.* **1992**, *104*, 692

[1] A. D. Bangham, R. W. Horne, *J. Mol. Biol.* **1964**, *8*, 660.
[2] J. M. Gebicki, M. Hicks, *Nature*, **1973**, *3243*, 232.
[3] W. R. Hargreaves, D. W. Deamer, *Biochemistry*, **1978**, *17*, 3759.
[4] H. Brockerhoff in *Bio Organic Chemistry, Vol. 3* (Ed.: E. E. von Tamelen), Academic Press, New York, **1977**, p. 1.
[5] C. Tanford, *The Hydrophobic Effect. Formation of Micelles, Polymers and Biological Membranes*, Wiley Interscience, New York, **1973**, Chap. 9.
[6] J. N. Israelachvili, D. J. Mitchell, B. W. Ninham, *J. Chem. Soc. Faraday Trans. 2* **1976**, 1525.
[7] T. Kunitake, Y. Okahata, *J. Am. Chem. Soc.* **1977**, *99*, 3860.
[8] A. W. Ralston, D. N. Eggenberger, P. L. DuBrow, *J. Am. Chem. Soc.* **1948**, *70*, 977.
[9] H. Kunieda, K. Shinoda, *J. Phys. Chem.* **1978**, *82*, 1710.

[10] G. W. Gray, P. A. Winsor in *Lyotropic Liquid Crystals* (Ed.: S. Friberg), American Chemical Society, Washington, **1976**, Chap. 1, p. 10.
[11] J. H. Fendler, *Membrane Mimetic Chemistry*, Wiley-Interscience, New York, **1982**, Chap. 6.
[12] J.-H. Fuhrhop, J. Mathieu, *Angew. Chem.* **1984**, *96*, 124; *Angew. Chem. Int. Ed. Engl.* **1984**, *23*, 100.
[13] H. Ringsdorf, B. Schlarb, J. Venzmer, *Angew. Chem.* **1988**, *100*, 117; *Angew. Chem. Int. Ed. Engl.* **1988**, *27*, 113.
[14] T. Kunitake, Y. Okahata, K. Tamaki, F. Kumamaru, M. Takayanagi, *Chem. Lett.* **1977**, 387.
[15] K. Deguchi, J. Mino, *J. Colloid Interface Sci.* **1978**, *65*, 155.
[16] U. Herrmann, J. H. Fendler, *Chem. Phys. Lett.* **1979**, *64*, 270.
[17] Y. Y. Lim, J. H. Fendler, *J. Am. Chem. Soc.* **1979**, *101*, 4023.
[18] K. Kano, A. Romero, B. Djermoune, H. H. Ache, J. H. Fendler, *J. Am. Chem. Soc.* **1979**, *101*, 4030.
[19] A. M. Carmona-Ribeiro, H. Chaimovitch, *Biochem. Biophys. Acta.* **1983**, *733*, 172.
[20] T. Kunitake, Y. Okahata, *Chem. Lett.* **1977**, 1337.
[21] T. Kunitake, N. Nakashima, S. Hayashida, K. Yonemori, *Chem. Lett.* **1979**, 1413.
[22] E. J. R. Sudhölter, J. B. F. N. Engberts, D. Hoekstra, *J. Am. Chem. Soc.* **1980**, *102*, 2467.
[23] Y. Murakami, A. Nakano, K. Fukuya, *J. Am. Chem. Soc.* **1980**, *102*, 4235.
[24] J.-H. Fuhrhop, H. Bartsch, D. Fritsch, *Angew. Chem.* **1981**, *93*, 797; *Angew. Chem. Int. Ed. Engl.* **1981**, *20*, 804.
[25] T. Kunitake, M. Shimomura, Y. Hashiguchi, T. Kawanaka, *J. Chem. Soc. Chem. Commun.* **1985**, 833.
[26] T. Kunitake, Y. Okahata, *Bull. Chem. Soc. Jpn.* **1978**, *51*, 1877.
[27] R. A. Mortara, R. H. Quina, H. Chaimovitch, *Biochem. Biophys. Res. Commun.* **1978**, *81*, 1080.
[28] Y. Okahata, S. Tanamachi, M. Nagai, T. Kunitake, *J. Colloid Interface Sci.* **1981**, *82*, 401.
[29] T. Kajiyama, A. Kumano, M. Takayanagi, Y. Okahata, T. Kunitake, *Contemp. Top. Polym. Sci.* **1984**, *4*, 829.
[30] K. Okuyama, Y. Soboi, K. Hirabayashi, A. Harada, A. Kumano, T. Kajiyama, M. Takayanagi, T. Kunitake, *Chem. Lett.* **1984**, 2117.
[31] K. Okuyama, Y. Soboi, N. Iijima, K. Hirabayashi, T. Kunitake, T. Kajiyama, *Bull. Chem. Soc. Jpn.* **1988**, *61*, 1485.
[32] K. Okuyama, N. Iijima, K. Hirabayashi, T. Kunitake, M. Kusunoki, *Bull. Chem. Soc. Jpn.* **1988**, *61*, 2337.
[33] H. Okada, Kyushu University, unpublished.
[34] M. Kodama, T. Kunitake, S. Seki, *J. Phys. Chem.* **1990**, *94*, 1550.
[35] Y. Okahata, R. Ando, T. Kunitake, *Ber. Bunsenges. Phys. Chem.* **1981**, *85*, 789.
[36] T. Kunitake, R. Ando, Y. Ishikawa, *Mem. Fac. Eng. Kyushu Univ.* **1986**, *46*, 221.
[37] J.-M. Kim, T. Kunitake, *Mem. Fac. Eng. Kyushu Univ.* **1989**, *49*, 93.
[38] M. Shimomura, T. Kunitake, *Chem. Lett.* **1981**, 1001.
[39] M. Shimomura, T. Kunitake, *J. Am. Chem. Soc.* **1982**, *104*, 1757.
[40] T. Kunitake, H. Ihara, Y. Okahata, *J. Am. Chem. Soc.* **1983**, *105*, 6070.
[41] For example V. Luzzati in *Biological Membranes* (Ed.: D. Chapman), Academic Press, New York, **1968**, p. 71.
[42] Y. Murakami, A. Nakano, J. Kikuchi, T. Takaki, K. Uchimura, *Chem. Lett.* **1983**, 1891.
[43] Y. Murakami, J. Kikuchi, T. Takaki, K. Uchimura, A. Nakamo, *J. Am. Chem. Soc.* **1985**, *107*, 2161.
[44] Y. Murakami, J. Kikuchi, T. Takaki, K. Uchimura, *Bull. Chem. Soc. Jpn.* **1986**, *59*, 515.
[45] L. A. M. Rupert, D. Hoekstra, J. B. F. N. Engberts, *J. Am. Chem. Soc.* **1985**, *107*, 2628.
[46] L. A. M. Rupert, J. B. F. N. Engberts, D. Hoekstra, *J. Am. Chem. Soc.* **1986**, *108*, 3920.
[47] L. A. M. Rupert, J. F. L. van Breemen, E. F. J. van Bruggen, J. B. F. N. Engberts, D. Hoekstra, *J. Membr. Biol.* **1987**, *95*, 255.
[48] A. M. Carmina-Ribeiro, H. Chaimovitch, *Biophys. J.* **1986**, *50*, 621.
[49] For example D. F. Evans, B. W. Ninham, *J. Phys. Chem.* **1986**, *90*, 226.
[50] H. Hotani, *J. Mol. Biol.* **1984**, *178*, 113.
[51] N. Nakashima, S. Asakuma, T. Kunitake, H. Hotani, *Chem. Lett.* **1984**, 227.
[52] N. Kimizuka, T. Takasaki, T. Kunitake, *Chem. Lett.* **1988**, 1911.
[53] T. Kunitake, Y. Okahata, *J. Am. Chem. Soc.* **1980**, *102*, 549.
[54] M. Shimomura, R. Ando, T. Kunitake, *Ber. Bunsenges. Phys. Chem.* **1983**, *87*, 1134.
[55] Y. Okahata, T. Kunitake, *Ber. Bunsenges. Phys. Chem.* **1980**, *84*, 550.
[56] Y. Okahata, H. Ihara, M. Shimomura, S. Tawaki, T. Kunitake, *Chem. Lett.* **1980**, 1169.
[57] T. Kunitake, Y. Okahata, M. Shimomura, S. Yasunami, K. Takarabe, *J. Am. Chem. Soc.* **1981**, *103*, 5401.
[58] M. Shimomura, H. Hashimoto, T. Kunitake, *Chem. Lett.* **1982**, 1285.
[59] T. Kunitake, R. Ando, Y. Ishikawa, *Mem. Fac. Eng. Kyushu Univ.* **1986**, *46*, 245.
[60] I. Cho, J. G. Park, *Chem. Lett.* **1987**, 977.
[61] T. Kunitake, N. Yamada, N. Fukunaga, *Chem. Lett.* **1984**, 1089.
[62] M. Kasha in *Spectroscopy of the Excited State* (Ed.: B. D. Bartolo), Plenum Press, New York, **1976**, p. 337.
[63] T. Kunitake, M. Shimomura, T. Kajiyama, A. Harada, K. Okuyama, M. Takayanagi, *Thin Solid Films* **1984**, *121*, L89.
[64] G. Xu, K. Okuyama, M. Shimomura, *Polym. Prepr. Japan* **1989**, *38*, 2407.
[65] K. Okuyama, H. Watanabe, M. Shimomura, K. Hirabayshi, T. Kunitake, T. Kajiyama, N. Yasuoka, *Bull. Chem. Soc. Jpn.* **1986**, *59*, 3351.
[66] H. Watanabe, K. Okuyama, H. Ozawa, K. Hirabayashi, M. Shimomura, T. Kunitake, N. Yasuoka, *Nippon Kagaku Kaishi* **1988**, 55.
[67] K. Okuyama, C. Mizuguchi, G. Xu, M. Shimomura, *Bull. Chem. Soc. Jpn.* **1989**, *62*, 3211.
[68] Y. Nakayama, T. Takahagi, F. Soeda, A. Ishitani, M. Shimomura, K. Okuyama, T. Kunitake, *Appl. Surf. Sci.* **1988**, *33/34*, 1307.
[69] A. Harada, K. Okuyama, A. Kumano, T. Kajiyama, M. Takayanagi, T. Kunitake, *Polym. J.* **1986**, *18*, 281.
[70] Y. Ishikawa, T. Nishimi, T. Kunitake, *Chem. Lett.* **1990**, 165.
[71] T. Kunitake, N. Kimizuka, N. Higashi, N. Nakashima, *J. Am. Chem. Soc.* **1984**, *106*, 1978.
[72] N. Kimizuka, H. Ohira, M. Tanaka, T. Kunitake, *Chem. Lett.* **1990**, 29.
[73] For example S. C. Kushwaha, M. Kates, G. D. Sprott, I. C. P. Smith, *Biochem. Biophys. Acta* **1981**, *664*, 156.
[74] Y. Okahata, T. Kunitake, *J. Am. Chem. Soc.* **1979**, *101*, 5231.
[75] S. Yasunami, Masters Thesis, *Kyushu University*, **1980**.
[76] E. Baumgartner, J.-H. Fuhrhop, *Angew. Chem.* **1980**, *92*, 564; *Angew. Chem. Int. Ed. Engl.* **1980**, *19*, 550.
[77] J.-H. Fuhrhop, H.-H. David, J. Mathieu, V. Liman, H.-J. Winter, E. Boekema, *J. Am. Chem. Soc.* **1986**, *108*, 1785.
[78] T. Kunitake, A. Tsuge, K. Takarabe, *Polym. J. (Tokyo)* **1985**, *17*, 633.
[79] T. Kunitake, Y. Okahata, S. Yasunami, *J. Am. Chem. Soc.* **1982**, *104*, 5547.
[80] T. Kunitake, S. Tawaki, N. Nakashima, *Bull. Chem. Soc. Jpn.* **1983**, *56*, 3235.
[81] T. Kunitake, N. Higashi, *Makromol. Chem. Suppl.* **1985**, *14*, 81.
[82] T. Kunitake, N. Higashi, *J. Am. Chem. Soc.* **1985**, *107*, 692.
[83] For example P. Mukerjee, A. Y. S. Yang, *J. Phys. Chem.* **1976**, *80*, 1388.
[84] T. Kunitake, N. Nakashima, M. Shimomura, Y. Okahata, K. Kano, T. Ogawa, *J. Am. Chem. Soc.* **1980**, *102*, 6642.
[85] T. Kunitake, N. Nakashima, K. Morimitsu, *Chem. Lett.* **1980**, 1347.
[86] N. Nakashima, S. Asakuma, J.-M. Kim, T. Kunitake, *Chem. Lett.* **1984**, 1709.
[87] N. Nakashima, S. Asakuma, T. Kunitake, *J. Am. Chem. Soc.* **1985**, *107*, 509.
[88] Y. Ishikawa, T. Nishimi, T. Kunitake, *Chem. Lett.* **1990**, 25.
[89] T. Kunitake, N. Yamada, *J. Chem. Soc. Chem. Commun.* **1986**, 655.
[90] K. Yamada, H. Ihara, T. Ide, T. Fukumoto, *Chem. Lett.* **1984**, 1713.
[91] J.-M. Kim, Y. Ishikawa, T. Kunitake, *J. Chem. Soc. Perkin Trans. 2*, **1991**, 885.
[92] P. Yager, P. E. Schoen, *Mol. Cryst. Liq. Cryst.* **1964**, *106*, 371, and subsequent publications by these authors.
[93] B. Pfannemuller, W. Walte, *Chem. Phys. Lipids* **1985**, *37*, 227.
[94] J.-H. Fuhrhop, U. Liman, V. Koesling, *J. Am. Chem. Soc.* **1988**, *110*, 6840.
[95] N. Wagner, K. Dose, H. Koch, H. Ringsdorf, *FEBS Lett.* **1981**, *132*, 313.
[96] P. N. Tyminski, L. H. Latimer, D. F. O'Brien, *Biochemistry* **1988**, *27*, 2696.
[97] I. Hamachi, S. Noda, T. Kunitake, *J. Am. Chem. Soc.* **1990**, *112*, 6744.
[98] I. Hamachi, S. Noda, T. Kunitake, *J. Am. Chem. Soc.*, **1991**, 113, 9625.
[99] Y. Murakami, J. Kikuchi, K. Akiyoshi, N. Shiratori, *Isr. J. Chem.* **1987/1988**, *28*, 23.
[100] Y. Murakami, Y. Hisaeda, T. Ohno, Y. Matsuda, *Chem. Lett.* **1986**, 731.
[101] T. Kunitake, *New J. Chem.* **1987**, *11*, 141.
[102] For example R. A. Moss, T. Fujita, S. Ganguli, *Langmuir* **1990**, *6*, 1197.
[103] M. Shimomura, T. Kunitake, *J. Am. Chem. Soc.* **1987**, *109*, 5175.
[104] N. Nakashima, R. Ando, H. Fukushima, T. Kunitake, *J. Chem. Soc. Chem. Commun.* **1982**, 707.
[105] T. Kunitake, Y. Ishikawa, M. Shimomura, *J. Am. Chem. Soc.* **1986**, *108*, 327.
[106] For example N. Kimizuka, T. Kunitake, *Colloids Surf.* **1989**, *38*, 79.
[107] S. Kato, T. Kunitake, *Chem. Lett.* **1991**, 261.
[108] N. Nakashima, R. Ando, T. Kunitake, *Chem. Lett.* **1983**, 1577.
[109] For example W. L. Hubell, H. M. McConnell, *Proc. Natl. Acad. Sci. USA* **1989**, *64*, 20.
[110] Y. Okahata, H. Ebato, *Anal. Chem.* **1989**, *61*, 2185.
[111] T. Kunitake, Y. Ishikawa, M. Shimomura, H. Okawa, *J. Am. Chem. Soc.* **1986**, *108*, 2059.
[112] Y. Ishikawa, T. Kunitake, *J. Am. Chem. Soc.* **1991**, *113*, 621.
[113] S. Asakuma, T. Kunitake, *Chem. Lett.* **1989**, 2059.
[114] S. Asakuma, H. Okada, T. Kunitake, *J. Am. Chem. Soc.* **1991**, *113*, 1749.
[115] K. Sakata, T. Kunitake, *Chem. Lett.* **1989**, 2159.
[116] K. Sakata, T. Kunitake, *J. Chem. Soc. Chem. Commun.* **1990**, 504.
[117] H. Okada, K. Sakata, T. Kunitake, *Chem. Mater.* **1990**, *2*, 89.
[118] Y. Ishikawa, H. Kuwahara, T. Kunitake, *J. Am. Chem. Soc.* **1989**, *111*, 8530.
[119] Y. Ishikawa, H. Kuwahara, T. Kunitake, *Chem. Lett.* **1989**, 1737.